GA-A15344
SAND 79-7015
UNLIMITED RELEASE
UC-62 DISTRIBUTION

INSTALLATION AND STARTUP OF THE FIXED MIRROR SOLAR CONCENTRATOR COLLECTOR FIELD SUBSYSTEM

FINAL REPORT FOR THE PERIOD JANUARY 31, 1977 THROUGH MARCH 31, 1979

by

G. H. EGGERS

Prepared by
General Atomic Company, San Diego, California
for
Sandia Laboratories
under Contract Nos. 07-7195 and 05-4569
and by
Sandia Laboratories, Albuquerque, New Mexico
and Livermore, California
for the
United States Department of Energy
under Contract AT(29-1)-789

DATE PUBLISHED: JUNE 1979

GENERAL ATOMIC COMPANY

Issued by Sandia Laboratories, operated for the United States Department of Energy by Sandia Corporation

Printed in the United States of America
Available from
National Technical Information Service
U.S. Department of Commerce
5285 Port Royal Road
Springfield, Virginia 22161
Price: Printed Copy $7.25; Microfiche $3.00

GA-A15344
UC-62

INSTALLATION AND STARTUP OF THE FIXED MIRROR SOLAR CONCENTRATOR COLLECTOR FIELD SUBSYSTEM

FINAL REPORT FOR THE PERIOD JANUARY 31, 1977 THROUGH MARCH 31, 1979

by

G. H. EGGERS

Prepared by
General Atomic Company, San Diego, California
for
Sandia Laboratories
under Contract Nos. 07-7195 and 05-4569
and by
Sandia Laboratories, Albuquerque, New Mexico
and Livermore, California
for the
United States Department of Energy
under Contract AT(29-1)-789

SANDIA REPORT No. 79-7015
GENERAL ATOMIC PROJECT 3285
DATE PUBLISHED: JUNE 1979

GENERAL ATOMIC COMPANY

ABSTRACT

This report describes the work done by General Atomic Company to design, fabricate, install, and startup the Fixed Mirror Solar Concentrator (FMSC) at Sandia Laboratories for the Department of Energy. Total system cost was \$773 per m^2. The system cost projection for a commercial plant is \$188.73 per m^2. At design conditions, with the oil inlet temperature at 245°C and the oil outlet temperature at 316°C, the peak system efficiency at noon was 36.8%.

CONTENTS

FIGURES

TABLES

INTRODUCTION AND BACKGROUND

This report describes the work done by General Atomic Company (GA) for Sandia Laboratories under Subcontract Nos. 05-4569 and 07-7195 during the period January 31, 1977, through March 31, 1979. The objective of this work was to detail design, fabricate, install, and startup a 260 m^2 (2800 ft^2) Fixed Mirror Solar Concentrator (FMSC) subsystem. This effort was performed as a part of Phase II of the Sandia collector subsystem program for Sandia's solar total energy test facility. Phase I of the GA program was done under Contract No. 02-7671D; it is reported in GA-A14209 (Rev) (Ref. 1) and GA-A14595 (Ref. 2). The Phase I effort developed the preliminary design of the FMSC collector subsystem.

Early in Phase II the Phase I collector design was reviewed, and the design was finalized with some minor changes made to increase performance. A 7.62 m (25 ft.) long experimental test module was then constructed, tested at GA, and disassembled and sent to Sandia where it underwent further testing.

The metal forms for casting the concrete modules were fabricated and assembled by the General Atomic shop, and fabrication of other hardware was performed by subcontractors. Casting of the concrete modules for the 260 m^2 (2800 ft^2) FMSC subsystem was done on site at Sandia, and the assembly and installation was done by local contractors under GA's supervision.

The project generally demonstrated the usefulness of construction experience in determining areas where improvements could be made in design and assembly procedures. It is believed that design changes and construction experience could substantially reduce future costs.

Subsystem startup began in January 1978 and the subsystem became completely operational in March 1978. A test program was conducted

throughout the startup period. On June 26, 1978, the design operating temperature of 316°C (600°F) was achieved and oil heated by the FMSC collector subsystem was used to make toluene vapor and generate electricity. Subsystem efficiency tests were conducted and for the design temperature resulted in estimates for noon-time efficiency of 35.4% near the summer solstice and 36.8% for December 5, 1978. These efficiencies are somewhat lower than expected, due principally to light spillage outside the aperture of the heat receiver. Performance could be substantially improved by tightening tolerances on the system optics.

EXECUTIVE SUMMARY

The Fixed Mirror Solar Concentrator (FMSC) subsystem installed at Sandia Laboratories in Albuquerque, N.M., has 260 m^2 (2800 ft^2) of collector aperture arranged in two 61 m (200 ft.) long rows. Each row contains sixteen 3.81 m (12.5 ft.) long by 2.18 m (7.17 ft.) wide concentrator modules, serviced by 7.62 m (25 ft.) long heat receiver sections. The heat receivers are connected in series, with a series crossover being used to connect the two rows.

The concentrator modules were constructed on site of steel fiber-reinforced concrete, and second surface glass mirror strips were attached to provide the reflective surface. The concrete is a substantial structure that is insensitive to high winds and provides solid attachment points for the heat receiver support structure.

The heat receiver assembly (HRA) was designed for use with Therminol 66 heat transfer fluid and includes a 25.4 mm (1 in.) by 63.5 mm (2.5 in.) rectangular cross section mild steel coolant tube with a black chrome selective coating. The tube is surrounded on three sides by high performance thermal insulation, and there is a window on the fourth side through which the concentrated sunlight passes. The HRA also includes a three-sided aluminum channel surrounding the insulation and two aluminum extrusions that form a secondary concentrator to further concentrate the sunlight reflected from the primary concentrator. The HRA was shop assembled and shipped to the site ready for installation.

Subsystem startup began in January 1978, and it became completely operational in March 1978. The subsystem has operated properly with the control system operating very well and the receiver tracking accurately. The fluid temperature control regulates the outlet temperature to

316°C ± 1.1°C (600.8°F ± 2.0°F) under test, although this part of the control system has not been extensively tested at this writing.

The peak subsystem thermal efficiency obtained to date was 36.8% on December 5, 1978, at design operating conditions, i.e., with the inlet oil temperature at about 245°C (473°F) and the outlet oil temperature at 316°C (600°F). The corresponding integrated daily efficiency is about 16%. The design peak thermal efficiency for the FMSC subsystem at Sandia is 50% for the equinoxes and 46% for the solstices. A peak efficiency of 42% was obtained for an experimental FMSC test module that preceded the startup of the full subsystem.

Although no direct measurement has been made to date for the receiver heat loss at the maximum operating temperature, the extrapolated value obtained from the lower temperature measurements is about 135 W/m^2 aperture or 273 W/m of receiver and crossover pipe. For a 1 kW/m^2 insolation, this is about 13.2% loss. This compares with heat loss measurements of about 6.8% made on the experimental test module which preceded the subsystem. The higher heat receiver thermal losses for the subsystem are attributed to additional piping for thermal expansion loops, downcomers, and the crossover, less thermal insulation in the heat receiver, and a larger coolant tube. The lower than expected subsystem efficiency is due primarily to light spillage at the heat receiver aperture caused by system misalignment and inaccuracies in the primary concentrator. Other factors include the higher than expected thermal loss from the receiver, and thermal insulation dust collecting on the inside of the heat receiver window, thus reducing light transmission through the window.

The project has demonstrated the operability of an FMSC subsystem at the 316°C (600°F) design outlet temperature, and has resulted in a first generation concentrator module being fabricated on site from precast concrete and glass mirrors. The basic approach is sound and is recommended for future ground-mounted FMSC applications.

The project has demonstrated the value of construction and operating experience by revealing ways in which the heat receiver, its support and drive components, the cast concrete and glass mirror concentrator module, and the concrete casting forms can be improved.

The first-time cost of fabricating the concrete modules was $70.80 per m^2 ($6.58 per ft^2) including the cost of the concrete, and the pouring, stripping, and cleaning of the forms. Experience gained on this project indicates that the concrete module cost could be reduced to about $37.66 per m^2 ($3.50 per ft^2) using the same methods.

FMSC subsystem cost projection studies were done on two levels: for the next plant and for a fully commercialized plant. This analysis assumed the next plant to have 9290 m^2 (100,000 ft^2) of aperture and be essentially of the same design as installed at Sandia. For the commercial plant, substantially the same assumptions were used, but with a commercial plant size of 92,900 m^2 (1,000,000 ft^2) and a production volume of 929,000 m^2 (10,000,000 ft^2) of aperture per year. The total installed costs (without a fee or profit allowance) for these two plants are given below:

Next plant	9,290 m^2	$448.19/$m^2$	($41.66/$ft^2$)
Commercial plant	92,900 m^2	$188.73/$m^2$	($17.54/$ft^2$)

Several key factors are expected to reduce costs, including larger aperture area for the module, and the use of mass production methods to reduce the labor requirement.

1. SYSTEM DESCRIPTION

The FMSC subsystem installed at Sandia Laboratories in Albuquerque, N.M., is illustrated in Fig. 1-1. The subsystem consists of two 200-ft-long rows of FMSC collectors with associated piping, valves, buffer tank, instrumentation, and controls. The FMSC subsystem was designed to be essentially an independent unit and the amount of interfacing with other portions of the Sandia system was minimal. The fluid system and control system interfaces were the only two interfaces that had to be integrated into Sandia's system. The FMSC subsystem was provided with the means for receiving warm Therminol 66 heat transfer oil from the Sandia main storage tank, heating the oil, and returning it to the main storage tank. It also is capable of operating in a recirculation mode in which the FMSC subsystem is valved off from Sandia's main system.

1.1. COLLECTOR

The collector includes the primary concentrator, the heat receiver assembly (HRA), and the HRA support structure and drive mechanism. The primary concentrator is the faceted mirror module, which is fixed, and its foundations and related components. The HRA includes the heat pipe, window, thermal insulation, secondary concentrator, and additional structural parts. The HRA support structure and drive mechanism hold the HRA above the concentrator and move it to track the focal line.

1.1.1. Primary Concentrator

The primary concentrator consists of the faceted mirror module. The substrate is a cast concrete unit with facets cast into the inner surface. Flat mirrors are bonded on these facets by means of a contact adhesive (3M Type 468). Each module is 3.81 m (12.5 ft.) long, with an aperture

Fig. 1-1. The FMSC collector subsystem installed at Sandia Laboratories' solar total energy test facility

width of 2.18 m (7.17 ft.), and contains forty-three 5.1 cm (2 in.) wide facets. The aperture is tilted 32 deg., corresponding to the latitude of Albuquerque, N.M. A module cross section is shown in Fig. 1-2. The modules are set on a foundation and lined up in an east-west row with the aperture facing south. For the subsystem two rows were used, each 61 m (200 ft.) long. The access spacing between the rows is 4.6 m (15 ft.) and the north row is elevated 15.2 cm (6 in.) higher than the south row to minimize the shadowing of the north row by the south row. Figure 1-1 shows the collector viewed from the east end.

Figure 1-3 illustrates the geometric properties of the FMSC. It contains a reference or tangent facet that is just tangent to the reference circle. The surface slopes of other facets then differ from the slope of the tangent facet by one-quarter of the included angle between a facet and the tangent facet.

The modules were cast on site at Sandia using a precision metal form. The 28-day setting strength of the concrete was 34,500 to 41,400 kPa (5000 to 6000 psi) and fiber re-enforcement was chosen to eliminate use of rebar and to homogeneously re-enforce the concrete to prevent crack propagation. As of this writing, it appears that no cracks are developing. The concrete contained 35.7 kg/m^3 (60 lb/yd^3) of 2.54 x 0.05 x 0.025 cm (1.0 x 0.02 x 0.01 in.) rolled steel fibers. Although the fiber concrete cost nearly three times the regular concrete, elimination of the re-enforcing bar resulted in a major saving in labor.

The foundations were designed for Sandia by the Allison Engineering Company. As a result of soil tests, the footings were set some 0.76 m (2-1/2 ft.) into the ground with piers forming the base for the module to set on. Each row was required to be level within 6.4 mm (1/4 in.). It turned out that the piers were actually within 3.2 mm (1/8 in.) of being level and straight.

The mirrors were made from Corning 0317 formulation glass. The selection of this glass was based on measurements made by Sandia on flatness and

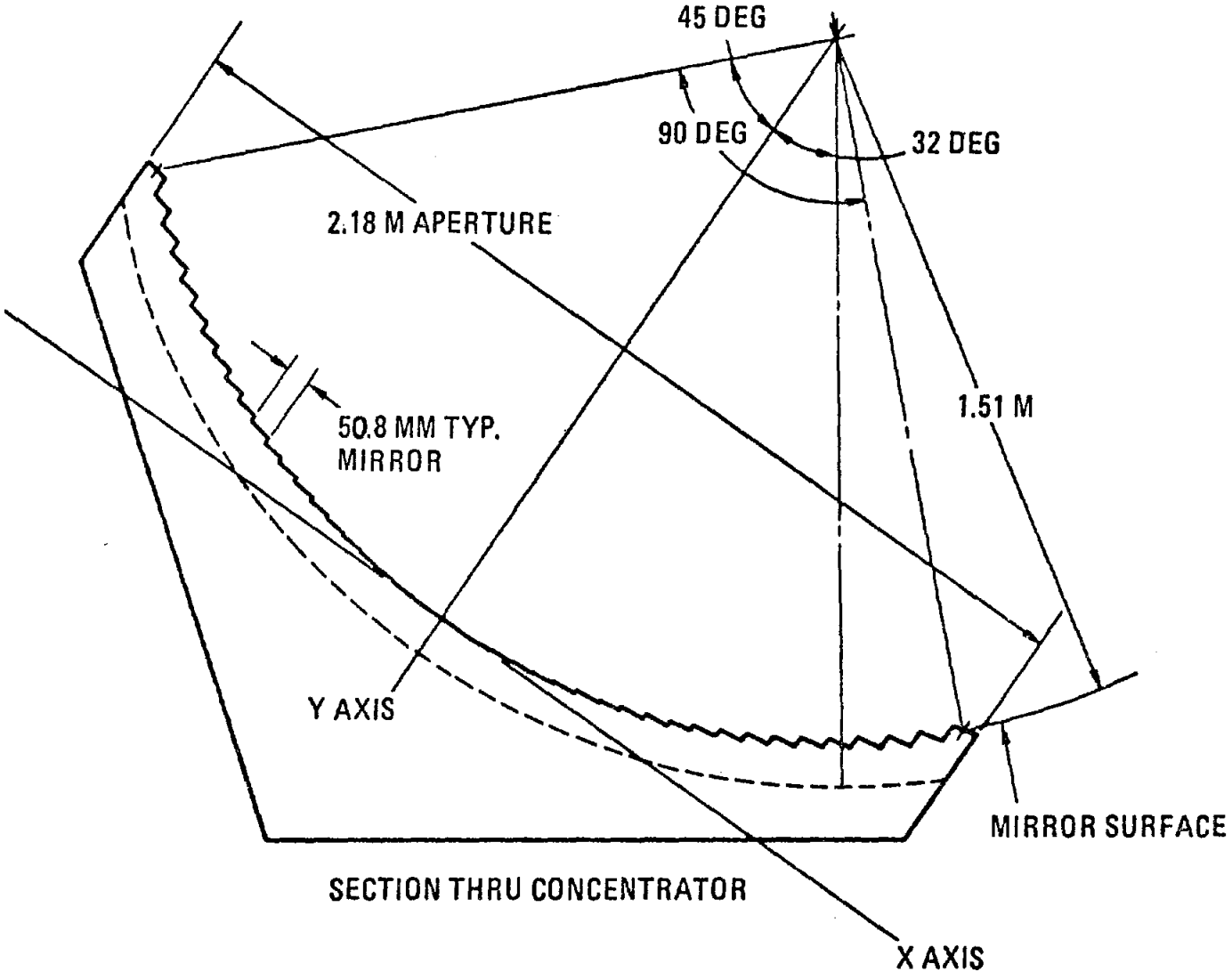

Fig. 1-2. Schematic diagram showing the cross section of the FMSC collector module

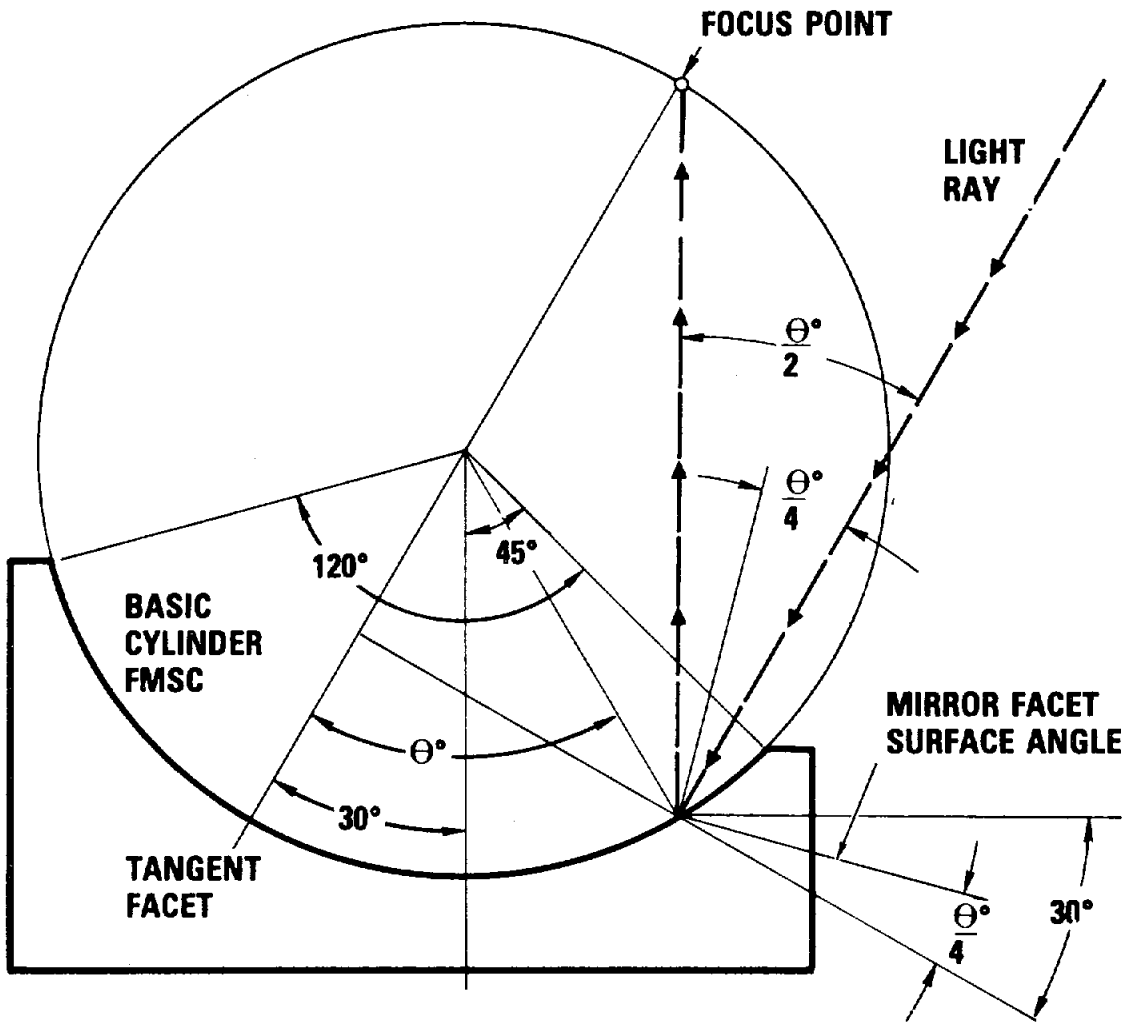

Fig. 1-3. FMSC geometric relationships

transmission. The project became aware of the availability of this glass through Sandia. The glass was 1.52 mm (0.060 in.) thick. It was silvered by a local mirror shop prior to cutting and the mirror reflectivity was measured to be 0.96 by Sandia Laboratories. The edges of the mirrors were seamed, and the backs were then coated with a polyurethane enamel. The mirrors were bonded to the concrete by 3M's No. 468 transferable adhesive.

Bonding the mirrors down individually by hand turned out to be an
.ve task. It is apparent that a more automated means must be devel-
) reduce labor costs.

Heat Receiver Assembly

The heat receiver assembly (HRA) was a unitized assembly that was pre-assembled in a shop and shipped to the site ready for installation.

The cross section of the HRA is shown schematically in Fig. 1-4. The major components are the support channel, the secondary concentrators, some side plate stiffeners (later removed), the heat pipe, the insulation, and the cover glass or Teflon. The support channel was a standard aluminum channel obtainable in 7.62 m (25 ft.) lengths. The secondary concentrator channels were extruded aluminum compound parabolic shapes. They served two purposes: (1) as a structural member and (2) as a secondary reflective surface for reconcentrating the light. The reflective surface was covered with Kinglux anodized aluminum 0.3 mm (0.012 in.) thick with a reflectivity of 0.88. The heat pipe was mild steel rectangular tubing 6.35 cm x 2.54 cm x 0.21 cm wall (2.5 in. x 1.0 in. x 0.083 in.). It was sized to ensure turbulent fluid flow and was electroplated on the outside with black chrome. The insulation was waterproofed, coated Microtherm imported from England; this is very fine cellular silica foam with a low thermal conductivity as shown in Fig. 1-5.

The heat receiver window is provided to reduce heat losses from the
: pipe, and was originally intended to be Pyrex glass. On the experi-
ental test module the Pyrex broke when the heat receiver was heated to

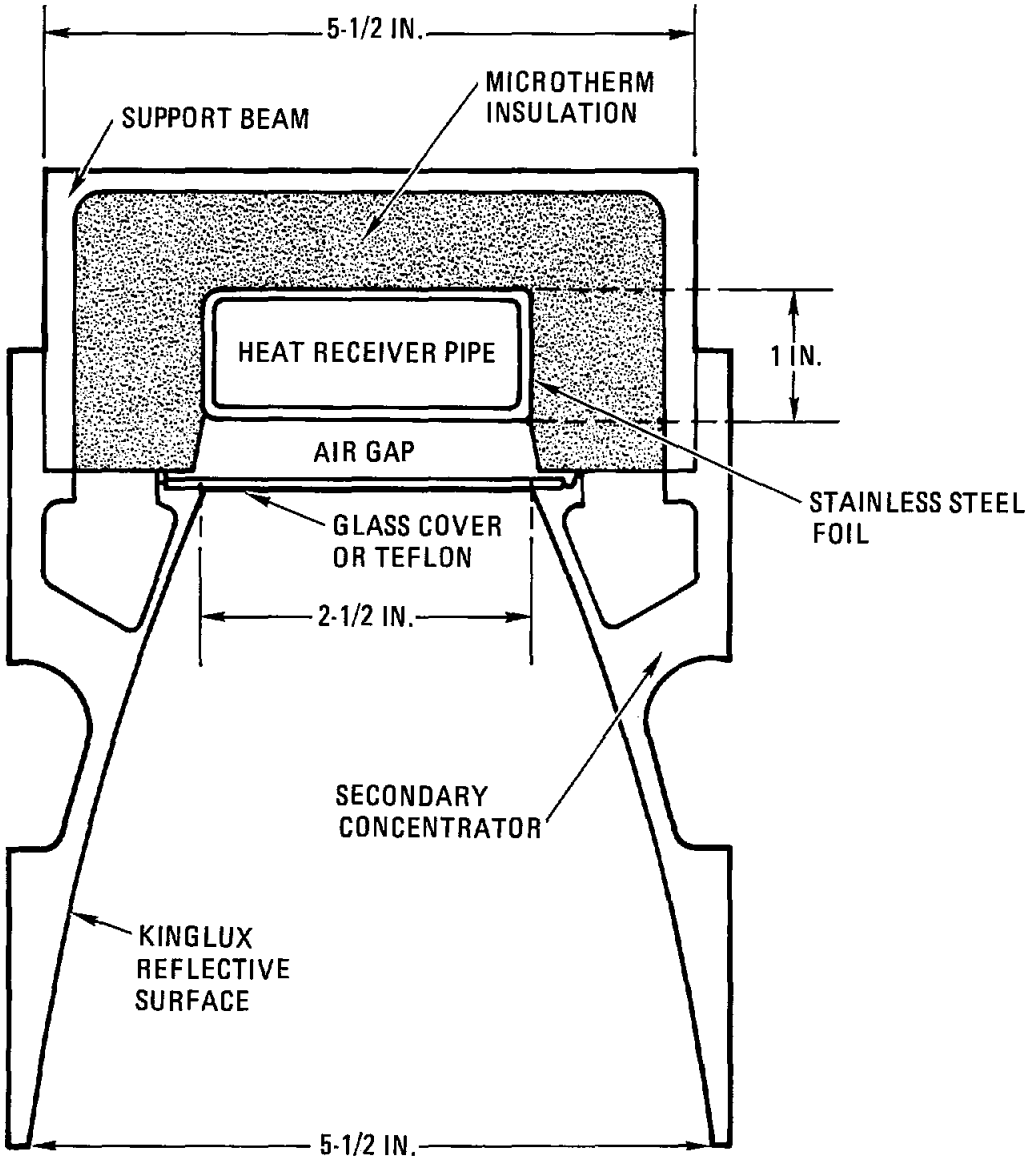

Fig. 1-4. Cross section of heat receiver assembly used on the FMSC collector subsystem

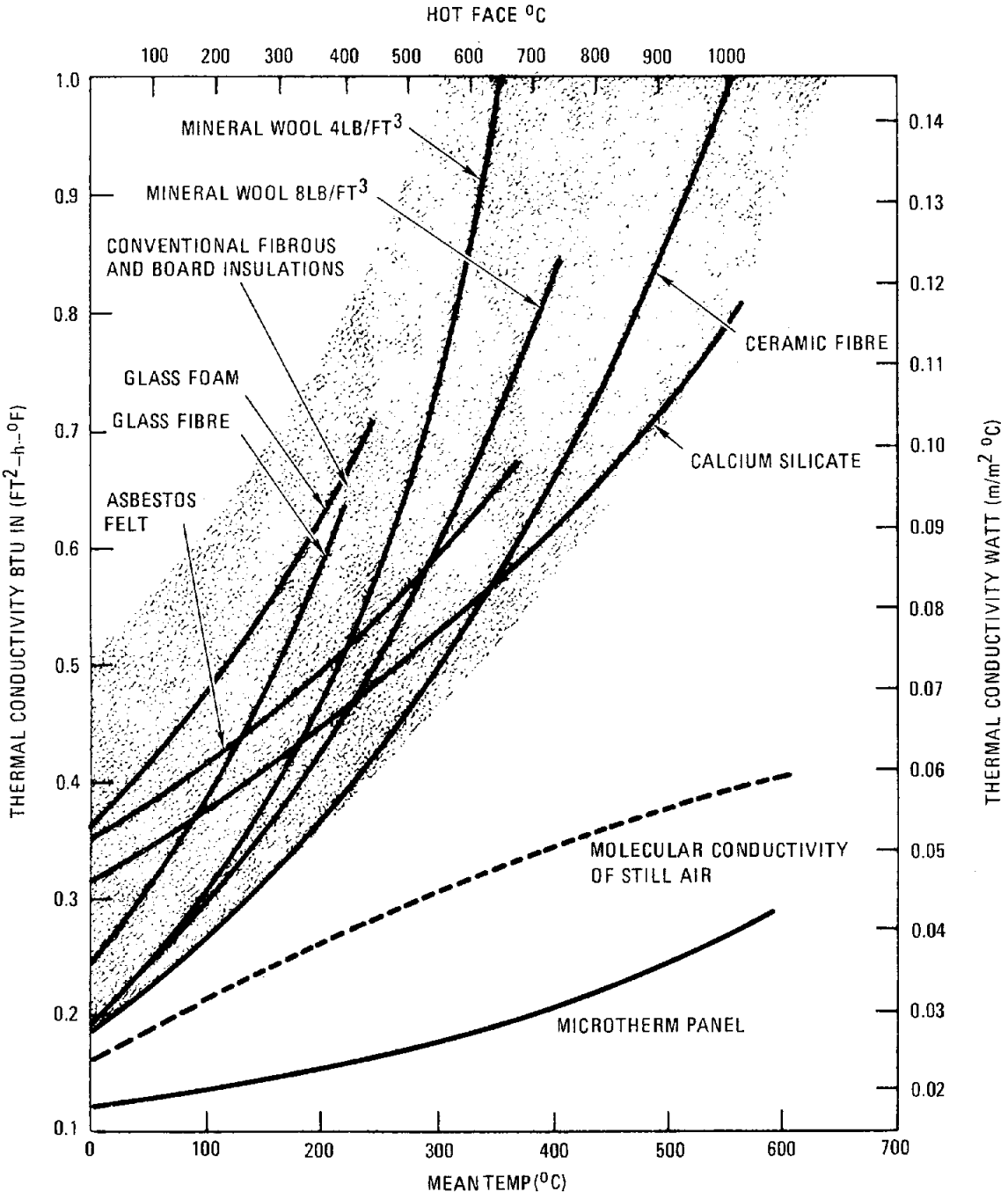

Fig. 1-5. Thermal conductivity comparison of different insulation materials

310°C (590°F). As a result, it was decided to use Teflon sheet for the window. The Teflon sheet used was 0.25 mm (0.010 in.) thick and had a transmissivity of about 0.94. However, it has to be installed with care so that it does not touch the pipe support rollers or the stainless steel foil or it will melt when the operating temperature is reached. If kept clear of these metal parts, it has performed satisfactorily with up to a 600°F fluid outlet temperature. The Teflon is also highly electrostatic and collects dust which, on its inner surface, is very difficult to clean.

The Kinglux polished anodized aluminum has performed satisfactorily at this writing. It has been very dirty and has been effectively cleaned with ammoniated window cleaner. Some spots of discoloration have been polished out without any apparent degradation of the reflecting surface.

Microtherm silica foam insulation is a very good thermal barrier, even though it is fragile, hard to seal, and when improperly sealed produces copious quantities of dust on the window. Other good insulators are also dusty, which means that in future designs insulation should be canned to prevent dusting.

The receiver sections were clamped together with Marman clamps. These clamps worked very well. On alternative receiver sections, a thermal expansion loop was used to absorb the hot pipe expansion, which was nearly 23 cm (9 in.) over the whole length. The loop was attached to the pipe by means of flange connections.

The receiver deflection due to sag was calculated to be about 1 cm (3/8 in.) when the receiver was in the vertical position and about 1.25 cm (1/2 in.) when it was in the horizontal position. The receiver operates close to the vertical position in the winter time, but it is below the horizontal position some of the time during the summer. The receiver was installed in the winter time and initial measurements showed that, at least

in the vertical position, the deflection was about as calculated. Later, with the summer bracket on and the receiver down to nearly horizontal, the maximum deflection was found to be nearly 3.8 cm (1-1/2 in.). This deflection caused considerable light loss and made alignment difficult. It was then decided to add some cable trusses with turnbuckle tensioners to the side of the receiver. The side plate was found not to have a measurable effect on the deflection, and so it was removed as the trusses were installed. When the trusses were installed and tensioned, the deflection was less than 3.2 mm (1/8 in.), but varied a little with receiver angle. The trusses were installed on only one side so as to straighten the receiver in the horizontal position. During winter operation, it may be necessary to reduce the tension or add a truss to the other side.

1.1.3. Heat Receiver Support and Drive Mechanisms

The support structure consists of two fixed members, one bolted to the back of the module and the other bolted to the front of the module. The mounting plates for these members attach two mirror modules together. The members are bolted to a common plate in the center of curvature of the module. Two flange bearings are mounted at the center pivot. A pivot bolt attaches the radial arm to these support members.

The tracking (or drive) mechanism consists of a motor, a speed reducer, 9 ball screw drives, and 11 interconnecting drive shafts for each collector row. The ball screw drives are attached to the radial arm by means of a bolt through a bronze bearing. The radial arm is rotated about its pivot by the rotating screw driving a ball nut back and forth along its length. The motor is a 1 hp dc permanent magnet motor with a variable speed controller. It can run up to 1800 rpm. The motor is coupled to the drive shafts by a 40:1 speed reducer. The drive shafts drive the worms of the ball nut drives, which drive the screw with a 6:1 speed reduction.

The receiver is mounted on the end of the radial arm by means of a split pillow block bearing. A guide rod attached to the center of the mirror and passing through a bearing on the side of the receiver keeps the receiver pointed at the tangent facet. All the receivers are keyed together by means of the "dumbbell" shafts that fit into the split pillow blocks.

The guide rod is a very simple and low cost means of keeping the receiver focused on the tangent facet, but it potentially hinders mechanical cleaning of the mirrors. Some other means of receiver support and tracking should be considered for future systems.

1.2. FLUID TRANSFER LOOP

A schematic of the fluid transfer loop of the FMSC subsystem is shown in Fig. 1-6. It consists of the delivery and return lines, the valves in these lines, a crossover or internal circulating valve, a buffer tank, pump, flow meters, piping, and the receivers. As the receivers are described in Section 1.1.3 as a separate unit, only the other parts of the fluid system are described here.

The fluid delivered from Sandia's low-temperature storage tank passes through the subsystem's buffer tank, through the pump and flow meter, and into the south row of receivers. At the other end of this row, the fluid passes through a crossover pipe to the north row of receivers and then is returned to Sandia's hot storage tank. The fluid pipe interface is at the junction pad bulkhead. On the Sandia side, a manual valve is located in both the supply and return line, and an air-powered valve in a crossover line. This permits Sandia to circulate hot fluid from their tanks to heat the oil lines, thereby preventing a cold slug of oil from entering the hot tank.

A flange connection connects the supply and return lines from Sandia's tanks to the supply and return lines to the collector. On the collector side, there is an air-powered valve in both the supply and return line and also in the crossover line. The supply line enters the buffer tank, which can be filled with oil from Sandia by simply opening the supply

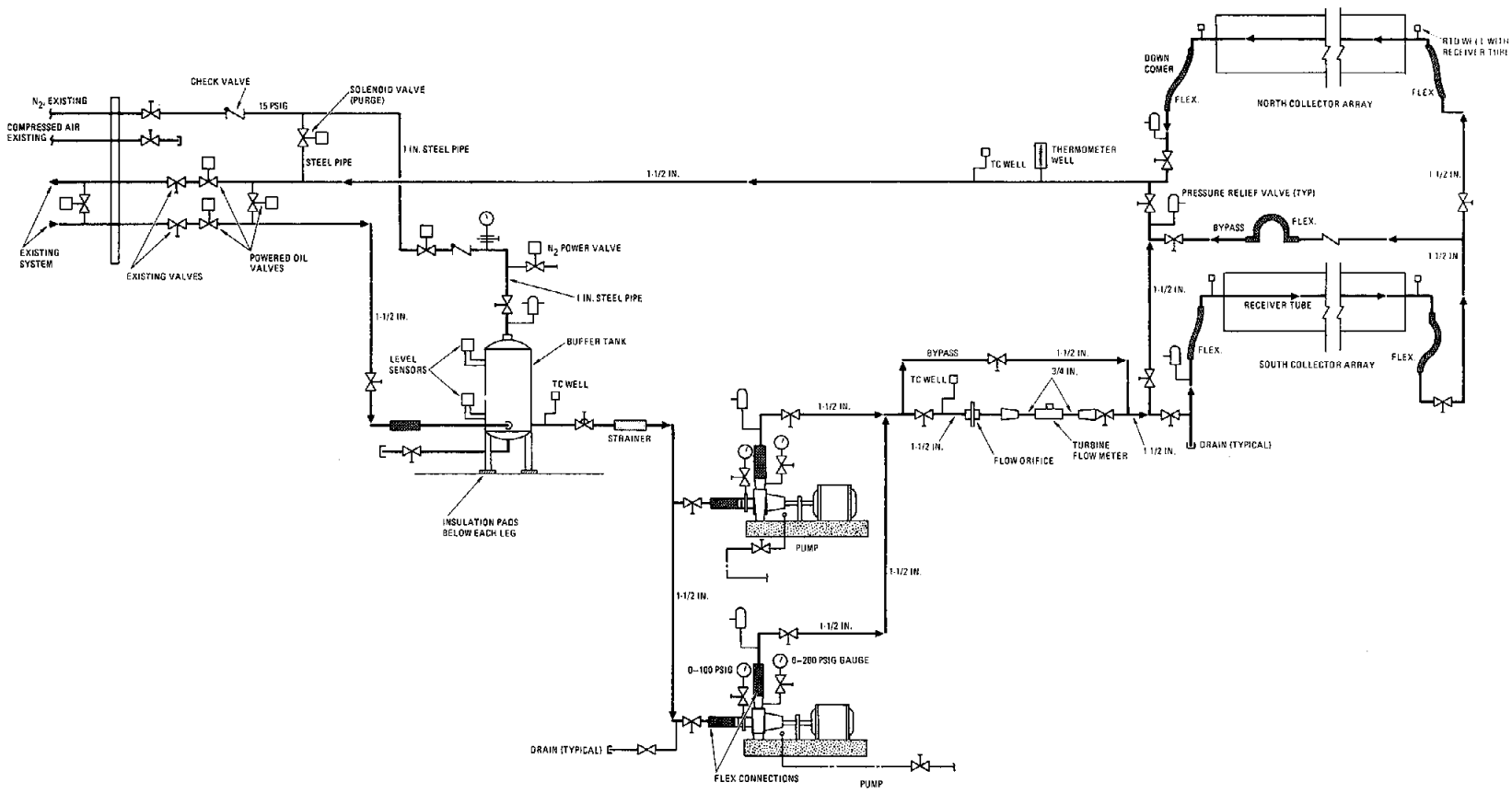

Fig. 1-6. Schematic diagram of the fluid transfer loop for the FMSC collector subsystem

valve and bleeding off the nitrogen pressure. From the buffer tank, the oil passes through a strainer and into the pump. By closing the supply and return valves and opening the crossover valve, oil can be circulated through the collector subsystem only. During startup, the collector system can be heated up to deliver oil to Sandia at the specified temperature.

The pump used is a Viking positive displacement gear pump driven by a 3 hp dc variable speed motor. This system is similar to Sandia's pumping system. The calculated pumping power is about 1/2 hp at operating temperature, so the motor is considerably larger than it needs to be. A second pump is installed to maintain operation if maintenance has to be performed on the first pump. The pumps can be isolated from each other. The pump has an internal relief valve, which limits the outlet pressure to 1242 kPa (180 psi). The operating pressure at ambient temperature is about 276 kPa (40 psig), and at 315°C (600°F) at the outlet the pressure drops to less than 69 kPa (10 psig).

Two types of flow meters are used to monitor flow. One is an orifice flow meter, which is read out locally on a gauge indicating inches of water pressure drop across the orifice. The flow is a constant times $\sqrt{\Delta P}$. The unit is calibrated for Therminol 66 at 250°C (481°F). It can be equipped with a transducer to transmit its data to a remote location. The local readout takes a long time to stabilize for accurate ΔP indications when the flow is changing. The other flow meter is a turbine type, which sends out a frequency proportional to the flow. This sensor is mounted in the fluid near the inlet end of the receiver, and its readout is located in the control room. It responds rapidly to changes in flow, and an in-line calibration showed that its error was within ±1%.

The system has a strainer in the exit line from the buffer tank. The strainer is a heavy wire frame for support with a 40-mesh screen for screening out foreign material. A permanent bar magnet is inserted in the screen to catch steel particles. During startup, a considerable amount of welding slag was cleaned out of the oil, mostly by the magnet. It appears that the magnet is by far the most effective trap for the steel particles.

The buffer tank was designed to contain the oil in the pipe. Its capacity, therefore, was about 340 liters (90 gallons) and about 262 liters (70 gallons) between the two level sensors, one for high- and one for low-level indication. If it is desired to purge the system, the oil in the pipe can be returned to the buffer tank. The buffer tank, therefore, has sufficient capacity for internal circulation, permitting system heatup during startup prior to transferring oil to the Sandia tanks.

Oil is received from the Sandia tanks and returned to them through two air-operated, remotely controlled valves. A similar valve is located in the crossover line to permit internal circulation. These valves can be operated locally, remotely, or automatically. In the automatic mode, they are opened when the outlet temperature reaches the desired level and are closed when the outlet temperature drops below a certain level. The crossover valve opens when the supply and return valves close, and closes when they open There are other manually operated valves for various functions in the fluid system.

The fluid system also has three remotely controlled, air-operated valves for controlling the nitrogen flow into the system. One of these vents the buffer tank, one supplies nitrogen to the buffer tank, and one supplies nitrogen to the outlet end of the heat pipe to blow the oil back into the buffer tank. While this is being done, the pump is run in reverse.

The piping of the fluid system is 3.8 cm (1-1/2 in.) mild steel schedule 40 pipe with welded fittings. Flanges are used wherever disconnects are required. The manual valves are all welded into the pipe. A flange disconnect is used to attach the flexible tube downcomers. The downcomers are connected to the heat receiver pipe by means of Marman clamps.

All the pipe and fittings were welded in the field. A number of problems were caused by poor fitting, burning holes through the pipe, leakage, and release of metallic particles inside the pipe. From this experience, it appears that shop welding as many pieces together as possible is the best approach to solve many of these problems. Also, for modest size systems,

preassembly using threaded fittings in the field followed by seal welding could eliminate the remainder of the problems. For large fields, maximum shop unit assembly with the field welding performed by portable automatic equipment is recommended.

1.3. INSTRUMENTATION AND CONTROL

The instrumentation is divided into two parts: measuring instrumentation and control instrumentation. For this system, a portion of the measuring instrumentation is also used for control. Instrumentation sensors used for data only are the orifice flow meter, the back side skin temperature thermocouples on the heat receiver pipe, one-half of the hot face skin temperature thermocouples, and two oil temperature thermocouples.

The instrumentation sensors used for control were the photo cells, the inlet and outlet temperature sensors*, and half the hot face skin temperature thermocouples. The turbine flow meter was used for a safety function as well as data, and the outlet fluid temperature thermocouple was used for valve switching as well as data.

The control instruments are located on the Sandia control panels in building 833. All of the control is accomplished through the control system. Manual control is provided at the junction pad through the motor control panels. Thermocouples are provided to supply data for the data recording computer in building 833.

1.3.1. Instrumentation

To take the data required to measure system performance, the fluid inlet and outlet temperatures and the flow rate are needed. The fluid temperatures at the inlet and outlet are measured by thermocouples inserted into the pipe. The thermocouples used are copper-constantan sheathed, and

*Resistance temperature devices (RTDs)

are inserted into the pipe through a ferrule-type fitting. These thermocouples can be either read out in the control room directly or entered into the computer, which will print out the data at desired intervals.

Four platinum RTDs in the fluid system, used primarily for control, were later adapted for data readout. One of these is on the inlet end of the receiver, two are at the midpoint (one on each row), and one is on the outlet end of the receiver. These RTDs were originally intended for control only, but after some operating experience it became clear that it would be very convenient to use them for data. Their input circuits to the control system were subsequently modified to permit direct readout.

The temperature of the hot face heat pipe is measured at five places: two places on the south row and three on the north row. One is near the inlet, one is near the midpoint, and one is near the outlet. The remaining two places are the midpoints of each row. There are two thermocouples at each place; one is copper-constantan and one is iron-constantan. These were all spot-welded to the pipe surface, but some were damaged and were repaired by brazing. These thermocouples provide skin temperature data. The copper-constantan set also provides safety control.

At these same places but on the back side of the pipe are located an additional set of thermocouples. These provide data only, and are the same as the front face thermocouples. These thermocouples, along with the hot face thermocouples, permit determination of the temperature gradient along the pipe as well as across it, i.e., exposed face to insulated face.

The flow information is provided by two flow meters. One is an orifice-type and the other is a turbine type. The orifice type simply measures the pressure drop across a given orifice and flow rate is obtained by multiplying the square root of this pressure drop by a constant. The orifice flow meter is designed and calibrated for measuring 249°C (480°F) Therminol 66. The pressure readout is local and is calibrated in inches of water. The gauge can be fitted with a transducer that will transmit the pressure reading to the control room.

The turbine-type flow meter with a magnetic pickup generates a pulse rate that is proportional to flow. Its readout is located in the control room. The readout unit has an output that provides a defocus signal if the flow rate reaches maximum and the outlet oil temperature rises above its operating level. This output signal, which is proportional to the flow rate, is also put into the computer for data printout. This flow meter has been accurate and troublefree. Although a voltmeter calibrated in percentage of full scale is used, another kind of meter could be employed. A digital readout in actual flow rate units is very convenient.

1.3.2. Control System

The control system is described in detail in Ref. 3. Only a functional description and operating experience are given here.

Figure 1-7 is a block diagram showing the control system functions. Figure 1-8 is a detailed functional diagram of the actual control system with the circuit boards being shown as blocks (A1, A2, etc., and L1, L2, etc.).

The control system performs three main functions:

1. It provides tracking control for the receiver by controlling the drive motor.

2. It regulates the outlet fluid temperature by controlling pump speed.

3. It provides safety functions.

The tracking control has two units: a coarse tracking unit and the fine or operational control unit. The coarse tracking unit (CTU) is mounted on a post on the equipment pad. In principle, it is a driven semicircular disk with photocells on each side of the disk. The motor drives the disk until the difference in the photo cell signal is zero, i.e.,

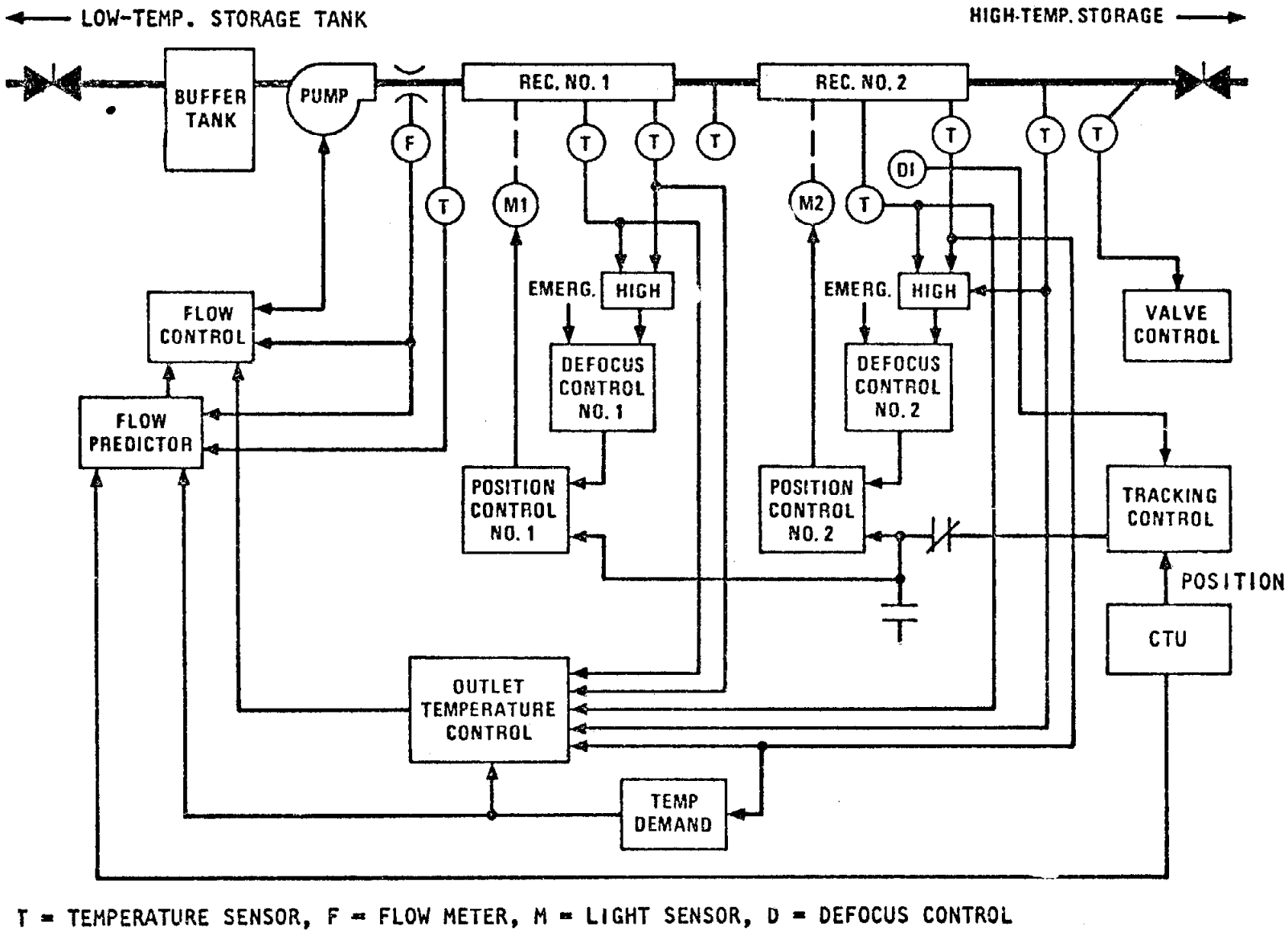

Fig. 1-7. Block diagram of the FMSC collector subsystem control system

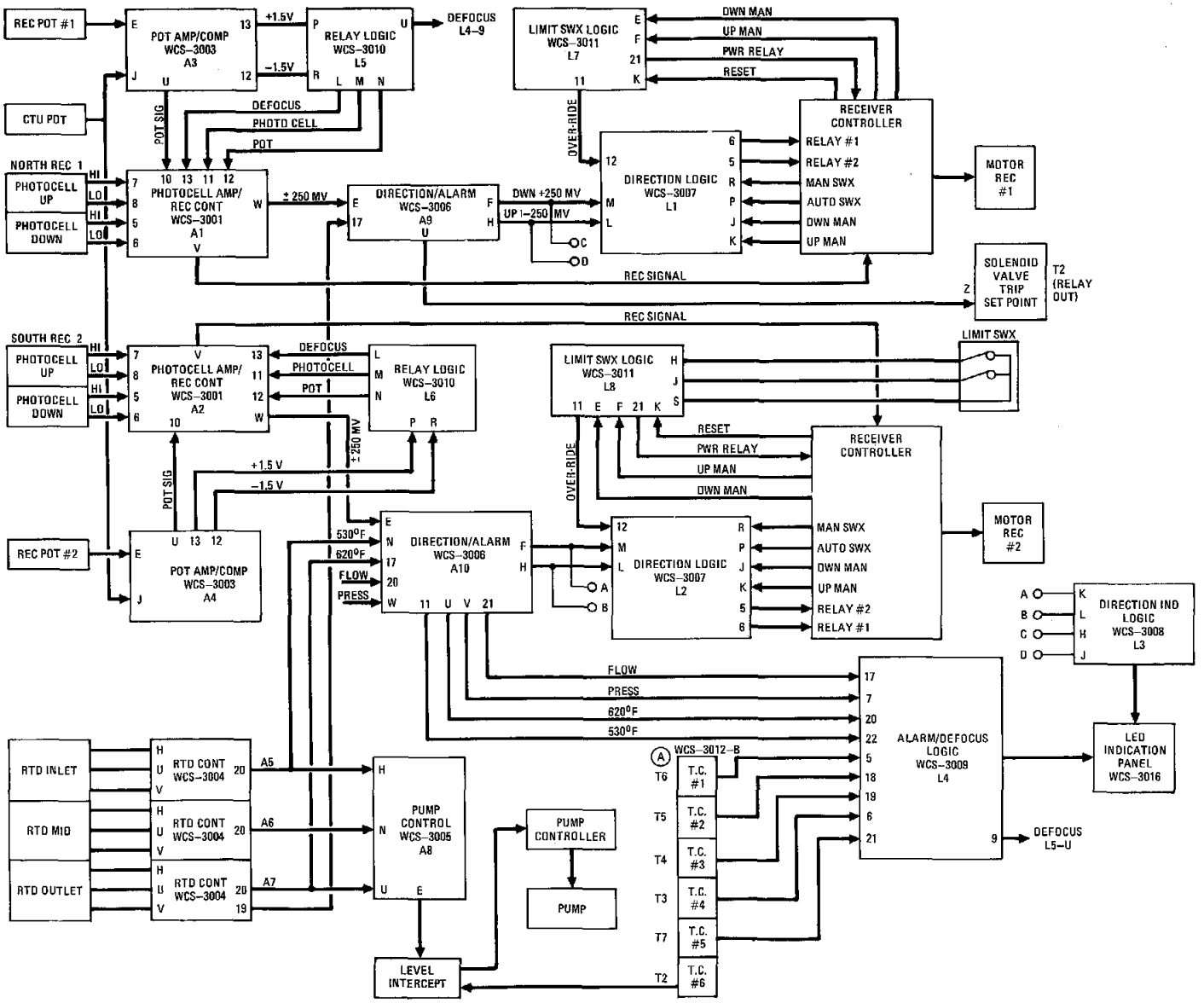

Fig. 1-8. Detailed functional diagram of the FMSC control system supplied by Western Control Systems

nulled. This motor also drives a potentiometer, which is coupled to a potentiometer that is locked to one of the radial arms. The receiver radial arm moves one half the angle of the CTU disk. The receiving tracking motor then drives the receiver until the difference in the signal from the CTU potentiometer and the radial arm potentiometer is zero. This brings the receiver to within 2.5 deg of the focal line and allows control to be taken over by photo cells mounted on the receiver.

The fine or operational tracking is controlled by receiver photocells mounted on the secondary concentrator at the edge of the secondary aperture. Each set consists of two cells, one mounted on each side of the aperture. The receiver is driven away from the cell producing the largest signal until the signals from the two cells are equal. The control circuits have voltage adjustments that can be set so the receiver continuously tracks, i.e., not by stepping.

The photocells can be adjusted to an optimum position to allow for irregularities in the focal line, or additional sets of cells can be installed and wired in parallel to provide an increased signal to allow for the lower signal in early morning and late afternoon. Experience to date shows that one set of cells on each row provides an adequate signal to maintain accurate tracking.

It was also learned that the CTU axis must be aligned with the receiver very closely, or a "crossing over" occurs in the morning and afternoon that shifts control over to the CTU because the signal from it overrides the photocell signal. If the CTU is properly aligned and the alignment with the receiver is set up at noon, the crossover problem disappears.

The fluid temperature control system works from signals provided by three platinum resistance thermometers. One of these is inserted into a thermowell at the inlet to the receiver, one is in the line at the midpoint, i.e., between the two rows, and the third is located at the outlet from the receiver. Each control circuit has a temperature "demand" potentiometer,

which requires the temperature to reach the "demand" level. The temperature rising above the demand signals the controller to speed up the pump motor, thereby increasing the flow rate, which, if the supply fluid is at constant temperature, will reduce the outlet temperature to its "demand" level. Similarly, if the outlet temperature drops below the "demand," it will signal the controller to reduce the pump motor speed allowing the outlet temperature to rise back to the demand level. The outlet temperature is primarily controlled by the outlet temperature controller when the inlet temperature is constant.

If the inlet temperature is variable, the inlet controller and midpoint controller provide signals that tend to vary the motor speed to compensate for the varying inlet temperature. This condition exists during startup.

Startup of the fluid circulation occurs in two steps. The fluid system contains a buffer tank, which has a capacity slightly in excess of the pipe volume. There also is an automatic valve in the oil supply line, the oil return line, and the crossover between them. During the first phase of startup, the oil supply and return valves (from and to Sandia's tanks) are closed and the crossover valve is open. Oil is circulated from the buffer tank through the system back to the buffer tank. The system is, therefore, preheated until the outlet oil temperatures reaches the required level. At that point, a signal from a thermocouple located in the outlet oil line triggers a command to the automatic valves which opens the supply and return valves and closes the crossover valve. During the switchover, temperature transients occur at the inlet; this affects the whole system and requires signals from the inlet and midpoint to prevent the outlet temperature from dropping too low or rising too high.

The control system also has a number of safety circuits that defocus the receiver under the following conditions:

1. Outlet oil temperature too high and flow rate maximum.
2. Inlet oil temperature too high.
3. Any one of five heat pipe skin temperatures too high.

If any one of the defocus circuits is active, a red LED lights up on the control panel, indicating the source of the defocus signal. When the receiver is in the defocus mode, it is driven 5 deg out of focus and follows the CTU with the 5 deg offset until the cause of the defocus is corrected.

The control panel also has functions that indicate the receiver position, the receiver motion, the minimum and maximum oil level in the buffer tank, and valve positions. There is also the capability for manual control as well as automatic control.

Nitrogen access is provided for both a gas cap on the oil and to apply pressure to blow the oil back into the buffer tank, i.e., purging the system. Pump reversal is also provided for purging the system.

2. SYSTEM CONSTRUCTION AND INSTALLATION

Construction and installation were performed in two discrete phases. One was the fabrication and testing of components and the second was the installation and assembly of the subsystem. The fabrication and testing phase consisted of parts and component procurement, fabrication of the components, assembling them into subassemblies and making acceptance tests. Major parts and components procured such as the pump, tracking motor, etc., were then shipped directly to Sandia to be installed. Component fabrication consisted of the support structure, drive tubes, and receiver components. The subassemblies were primarily the receiver, which was assembled as a unit ready for installation. The fabricated components and subassemblies were shipped to Sandia for installation. The forms for casting the mirror modules were assembled and tested at GA, and then shipped to Sandia where the subsystem modules were poured.

The installation phase consisted of construction of the module foundations or footings, the equipment pad, installation of the modules on the footings, and installation of the support structure, drive mechanism, receivers, fluid system and control system.

2.1. COMPONENT FABRICATION

The major components that had to be fabricated are listed below.

1. Concrete forms for casting the modules.
2. Receiver support structure.
3. Drive or tracking mechanism.
4. Receiver.
5. Fluid system - other than receiver.
6. Control system.

2.1.1. Forms

The first major component to be fabricated was the forms for casting the concrete modules. They were a costly item and required high precision. Also, they had to be made first so that the modules could be cast and ready for installation on schedule.

The forms were fabricated from extruded aluminum channels. The facet were machined on the web, which had been extruded extra thick to date these angles. As the variation of the width of the channel as d was 0.013 cm (±0.005 in.), the sides were also machined to narrow th tolerance. Machining the sides stress relieved some of the channels, which resulted in a longitudinal twist that had to be taken out. The channels were then placed on a precision machined template, as shown in Fig. 2-1, and riveted together. A special tangent facet channel was put in to facilitate stripping the form. This channel was to be pulled out and reinserted by screws. A framework was built into the form to hold the structure in place and permit it to be disassembled and reassembled without losing its shape. Forms for the module legs were bolted onto the sides, and covers for containing the concrete were attached on top of the form (the bottom of the module). The assembled form was then placed on the template and the facets were inspected with respect to the template by feeler gauges. The forms were then cleaned, primed, coated with Teflon and air dried. The form was tested by pouring a test module.

The forms worked well, but the screws incorporated to pull the tangent facet out could not be operated easily, and therefore this feature was not used in casting the modules at Sandia.

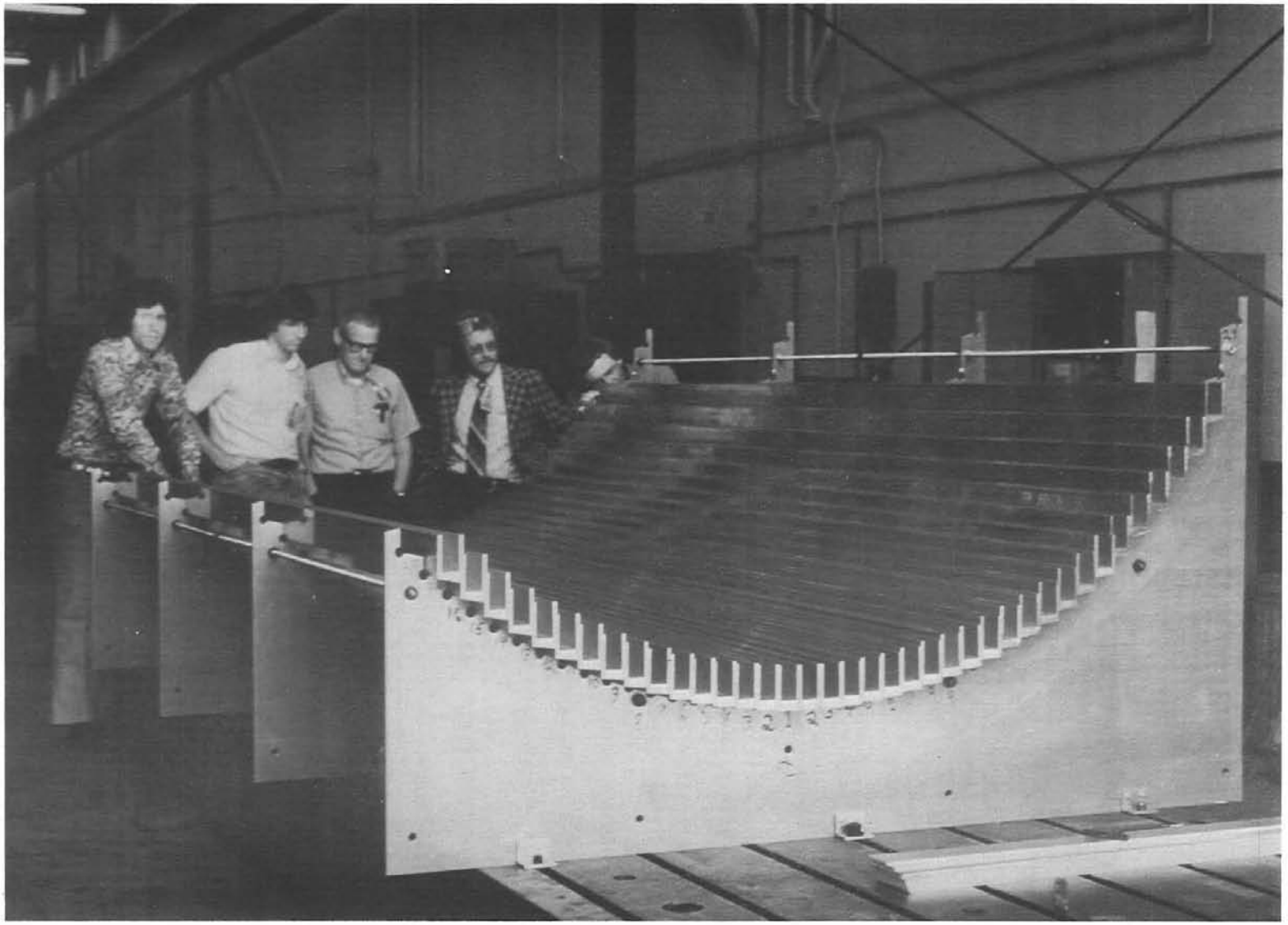

Fig. 2-1. Concrete form being assembled in GA shop

2.1.2. Heat Receiver

The receiver was assembled as a unit ready for installation into the subsystem. Fabrication of parts for the receiver included the aluminum extrusions for the secondary concentrator, the heat pipe, and the insulation. The remaining parts were purchased and assembled into the receiver. The extrusions for the secondary concentrator were of the Winston compound parabolic concentrator shape. Two extrusions were required for each receiver. They were bolted to a commercially available aluminum channel. These three pieces also made up the support beam.

The heat pipe was fabricated from 2.54 cm x 6.35 cm x 0.21 cm wall (1 in. x 2-1/2 in. x 0.083 in. wall) rectangular tubing of cold rolled steel electrically welded (1010 CREW). The tube was initially fabricated in two pieces with the transition from rectangular to round welded on one end of one piece and one end of the other piece welded shut. The fittings for the Marman clamps and for the thermal expansion loops were welded in place. Each unit was checked for leaks and then sent to the Highland Plating Company to be electroplated with black chrome coating. After each half was plated, they were welded together to complete the heat pipe assembly.

The quality of the coating was monitored at the vendor's site by Sandia personnel using Sandia's instruments for measuring the coating parameters. The absorptance averaged 0.97 ± 0.008, and the emissivity at 300°C (572°F) averaged 0.23 ± 0.014. The instruments used were the Gier-Dunkle mobile reflectometer, Model MS-251, for the absorptance, and the Model DB-100 infrared reflectometer for the emittance. Plating that did not measure close to this average was stripped off and the tube replated. Only three tubes turned out marginal, and they were replated. The detailed report of the Sandia personnel making these measurements is given in Appendix A.

The plated tubes were returned to the receiver assembly vendor, who welded the two halves together and finally leak-checked the pipe. The receiver assembly began with the supporting channel. The Microtherm

insulation blocks were inserted into the channel. The heat pipe was then inserted into the channel cut into the Microtherm for the pipe. A layer of 0.025 mm (0.001 in.) thick stainless steel foil was put between the Microtherm and the heat pipe to reduce rubbing on the Microtherm by the pipe when it thermally expanded. The Microtherm had also been wrapped in a fine glass cloth, which was then impregnated with a sodium silicate high temperature bonding agent. After the pipe was installed, the pipe support pins were installed.

The secondary concentrator extrusions did not have a high enough reflectance to be used as they were. Kinglux, a polished anodized aluminum sheet 0.3 mm (0.012 inch) thick was bonded to the parabolic surfaces by means of 3M's Type 468 contact adhesive. After the Kinglux was bonded to the extrusions and the Teflon window installed, the extrusions were installed on the channel. The Kinglux polished surface was protected with a thin plastic sheet bonded to it. This was removed prior to subsystem startup. The end plates for the receiver were then installed. Also, the guide rod bearing and bearing plate were installed after assembly.

2.1.3. Heat Receiver Support and Drive Mechanisms

Manufacture of the receiver support structure was contracted out to a vendor. This structure consisted of the mounting plates that were bolted onto the concrete module, two support members, the pivot bearing and the radial arm. The end of the radial arm included a mounting block for the receiver support pillow blocks. The pivot bearing support plate was preassembled as a unit.

The drive mechanism included the ball screw drives (or jacks), the drive tubes (or torque tubes), and the ball nut extension tube. The jacks were purchased and delivered to the vendor, who attached the ball nut extension tube. The torque tubes were made from 10 cm (4 in.) diameter aluminum irrigation tubing by simply welding an end plate into the tube end. The shaft assemblies, which coupled to the jacks, were bolted onto the end of the torque tubes and delivered as an assembled unit.

2.1.4. Fluid Transfer Loop

The only component fabricated for the fluid system was the buffer tank. The tank was fabricated to the ASME pressure vessel code. It was designed for 1035 kPa (150 psig) and was leak-tested at that pressure. Its total capacity was about 340 liters (90 gallons) with about 262 liters (70 gallons) capacity between the low level and high level sensors.

The remainder of the fluid system was assembled on site. The components were catalog items, which were installed during the fluid system installation. The fluid piping was all welded in place, and as many of the valves and other equipment were welded into the pipe as could be accomplished without making maintenance too difficult.

2.1.5. Control System

The control system was designed and fabricated by the vendor, Western Control Systems. The design effort consisted of taking a conceptual design, putting it into fabrication drawings, and specifying all the hardware components. The major part of fabrication design was in the circuit boards for the control channels. The circuit boards were designed and fabricated from the basic schematics. The boards were then assembled with standard, readily available parts whenever possible. This facilitated later maintenance and repair.

The card files, motor controllers, and cabinets were purchased as standard units. These were assembled into the total control system. A preassembly for bench testing was done with simulated input signals. As many adjustments and calibrations as possible were made prior to shipping the system to Sandia.

2.2. COMPONENT TESTING

Most of the component testing and verification were performed under the Phase I effort and reported in Refs. 1 and 2. However, some testing was continued under Phase II of this project. These tests included the following:

1. Evaluating the performance of a polyurethane enamel as a coating to protect the mirror silvering.

2. Checking the module forms by making test pours.

3. Bench testing the control system components.

2.2.1. Mirror Coating Tests

Previous mirror coating tests are described in Refs. 1 and 2. During Phase II additional samples were prepared and placed in Sandia's environmental test chamber. These samples were prepared using the method employed with the mirrors of modules for the FMSC subsystem. It involved seaming the edges (grinding) and coating the edges and back of the mirror with polyurethane enamel.

The process of seaming the edges is not lengthy or difficult, and the polyurethane enamel can be sprayed on; this is a low-cost method that is also compatible with mass production techniques. These factors make this treatment of the mirror attractive.

The tests conducted in the environmental test chamber exposed mirrors bonded to concrete blocks to 8-hour temperature cycles from -24.5°C (-20°F) to 54.4°C (130°F) and relative humidity from about 20% to 80% as shown in Fig. 2-2. None of the enamel peeled in the test chamber, although some chipping of the composite coating (silver, copper enamel, and polyurethane) was observed after extended exposure.

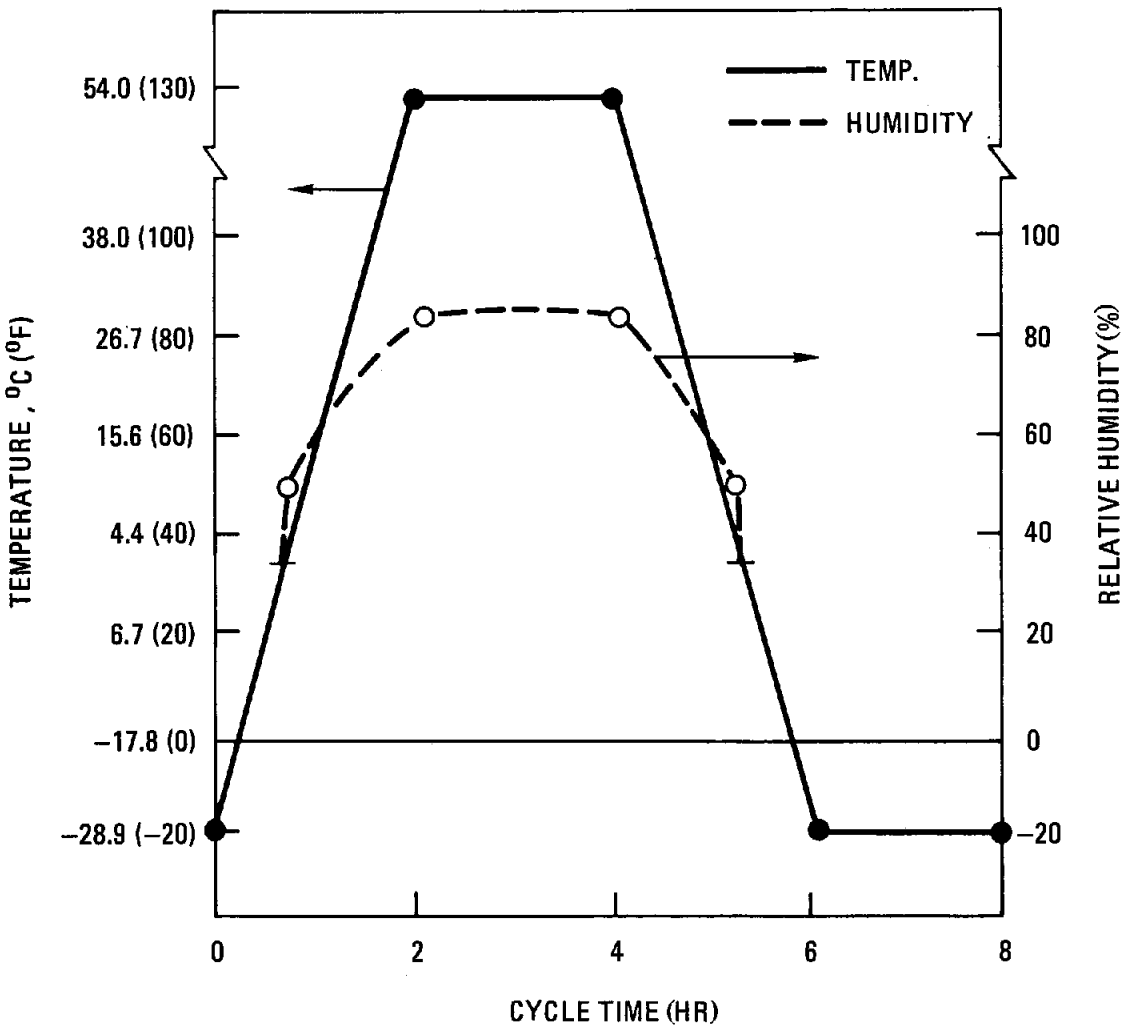

Fig. 2-2. Temperature and humidity as a function of time in the Sandia environmental test chamber for one cycle

The field experience gained to date, however, indicates that the polyurethane enamel will deteriorate and peel off under extended exposure to ultraviolet light. An ultraviolet-resistant material, such as one having a silicone base, should perform better.

2.2.2. Form Tests

Test modules were cast at General Atomic in each of the production forms to determine fabrication or design errors and to work out a casting procedure for casting the 32 modules of the subsystem. This experience resulted in the decision not to use the feature in the form that allowed the tangent facet channel to be lifted separately before pulling the rest of the form.

The concrete for the test modules, a five-bag mix of very low slump (too much water) was tested at 19,320 kPa (2800 psi). Instead of steel fiber, the test modules used a small amount of reinforcing bar. No problems were experienced when care was taken in handling. However, one test module was bumped fairly hard while it was being unloaded at Sandia, and a piece broke off. Use of fiber reinforcement, however, prevents breakage of this type.

2.2.3. Control System Tests

Control system fabrication was contracted out to a specialist in small electronic systems. This vendor performed a number of bench tests under simulated conditions to confirm operation of the components of the system. His final test confirmed bench operation of the electronic system under simulated input signals. The drawback of this test was that all the interconnecting wiring had to be disconnected and then rewired into Sandia's wiring system. Errors were made in the rewiring that were later corrected.

2.3. SYSTEM INSTALLATION

The subsystem was installed on the southeast quadrant of the solar total energy test facility. The area covered by the collectors is about 61.2 m (200 ft 9 in.) long and about 6.7 m (22 ft) wide. An additional area about 3 m (10 ft) by 6.7 m (22 ft) is used for the equipment pad, J-boxes, and holdup sump. Figure 2-3 is a schematic of the site layout.

The foundation was designed by the Allison Engineering Company. Sandia plant engineering department personnel reviewed the design and set the standards for the foundations. They also conducted soil tests and set the design specifications on the results of these tests.

The foundations consisted of a footing approximately 0.61 m wide x 1.83 m long (2 ft wide by 6 ft long) and 10 cm (4 in.) thick, and they were about 0.9 m (3 ft) deep in the ground. On these footings, a pier was poured for supporting the modules. The pier is 33 cm (13 in.) wide by 1.65 m (65 in.) long. Each pier, except the row ends, supports the end of two adjacent modules. Each row contains 17 piers for supporting 16 modules. The collector was installed level, which made the top of the footing about 10 cm (4 in.) below the pavement level on the east end and about 76 cm (30 in.) above the pavement level on the west end. There is no need for the collector rows to be level in the longitudinal direction, and a slight grade would be beneficial to draining; therefore, future systems will probably follow the terrain slope to some degree.

The concrete forms were shipped to Sandia after the test pours were completed. The forms were cleaned and reassembled prior to shipping. At Sandia, the vibrating support base was set on heavy, rubber-mounted pads and leveled. The form was then set on it. The form was not rigidly attached to the vibrating base. Heavy, air-driven vibrators were attached to the vibrating base to vibrate the form while the concrete was being poured. Probe type or "stinger" vibrators were also used to flow the wet concrete.

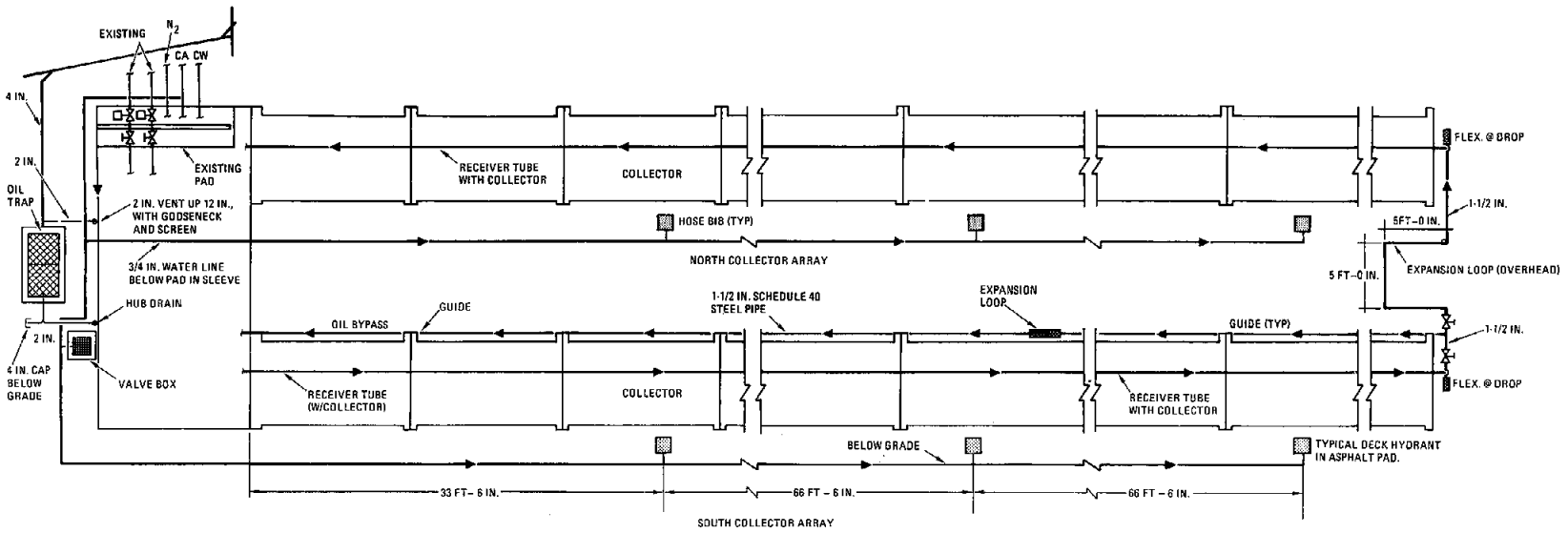

Fig. 2-3. Schematic layout of the FMSC collector subsystem

The concrete mix was about as follows:

1. 8 bags of cement per cubic yard of concrete.
2. 60 lb of steel fiber per cubic yard of concrete.
3. 1 cm (3/8 in.) aggregate.
4. Only enough water for high slump.
5. 55,000 kPa (8000 psi) estimated strength.

The forms were coated with a bond-breaking form oil prior to each pour.

The concrete supplier mixed the dry mix the evening before the concrete was to be delivered. Addition of the steel fiber required considerable effort on his part because the fiber had to be vibrated free and fed into the mix slowly and uniformly. Failure to add the fiber properly results in ball formation, which detracts from the effectiveness of the fiber and weakens the concrete structure. The fiber replaces the reinforcing steel that otherwise would be needed. The steel fibers are U-shaped and are 25.4 mm (1 in.) long by 0.5 mm (0.02 in.) wide and 0.25 mm (0.01 in.) thick rolled steel. The concrete was mixed as dry as possible. It actually came too dry to flow adequately into the form and additional water had to be added to make the concrete more fluid. The original test strength was expected to be about 55,200 kPa (8000 psi), but was reduced to 34,500 to 41,400 kPa (5000 to 6000 psi) after the addition of water.

Seven pours took place, with the modules poured in groups of five. Each pour required 7.6 m^3 (10 cubic yards) of concrete for an average of 1.5 m^3 (2 cubic yards) per module. The pours were started about 7:00 a.m. when the concrete trucks arrived. The first group pour was completed by about 11:00 a.m.; the last one was completed before 9:00 a.m. indicating that the learning process had increased productivity. The concrete set very quickly because of the rich mixture and the use of quick-setting cement. The top half of the form was stripped the same day and the form was pulled from the module the next day on the last three pours. The first pour was allowed to set over the weekend, which resulted in the module gripping the

form very tightly due to the concrete shrinking as it set. The concrete stripped away from the form cleanly, forming perfectly flat, smooth facets except for some facets close to and on either side of the tangent facet. On these facets, the concrete shrinkage caused the form to grip tightly enough to break the edges of some of the facets. These edges were subsequently repaired and smoothed to the adjacent surface. However, some precision was lost as a result. The design of future forms of this type should pay close attention to draft angle.

Since the modules were poured as the foundations were being built, they had to be stored until they could be installed on the foundations. The modules were completed about the same time the foundations were. A large forklift was used to handle the forms, strip them, and move the modules around. This technique worked well. Soon after the forms were stripped the modules were sprayed with concrete sealer.

As the modules were being installed, it soon became apparent that they would have to be shimmed to get the proper alignment. The leg portions of the form had sagged and were not as precise as needed, which resulted in uneven module legs. The foundations, however, were aligned to within 0.32 cm (±1/8 in.) of being straight and level. Shimming the modules was time consuming and pointed out the need, in the future, to cast the legs precisely or install adjustment screws in the modules for alignment.

After the modules were all set in place, the support structure base plates were installed. The shimming was done at this time so that both the mechanical system and the mirrors were well aligned. The support members and radial arms were installed, and a final alignment check was made of the radial arm pivot bearing. The ball screw drives were mounted next and attached to the radial arms, after which the torque tube drive shafts, gear reducer, and motor were installed. When each row was fully installed, aligned, and checked, the bases were grouted in so that the modules would be well supported.

Utility power and water were installed for each collector row. Three water hose connections and three 110-volt power outlets were installed under the south edge of each receiver row. The water outlets, which were of the freeze proof type, proved to be useful for cleaning the mirrors and maintaining the collectors.

The receivers were installed after the support structure was aligned and checked. The first receivers could not be installed as planned; it was impossible to connect up the Marman clamps with the receiver in place. The problem was that the clearance between the Marman clamp and the support shaft was inadequate to allow the flange to be inserted in position. An additional hole was therefore drilled in the end plate to raise the receiver pipe with respect to the support shaft. This permitted the Marman clamps to be connected. When the receivers were all connected together and leak-tested, they were lowered to the proper position.

The piping, buffer tank, pump pressure relief valves, and control valves were all installed in parallel with the receivers. When the installation was completed, the system was operated. An initial leak test was made with nitrogen at 414 kPa (60 psi). After preliminary operation and having checked the system up to about 204°C (400°F) oil temperature, a hot oil pressure test was conducted during which Sandia personnel filled the system with hot oil and pressurized it to 1380 kPa (200 psi). No leaks were detected and no failures occurred. This pressure was about twice the maximum expected operating pressure under worst conditions, and was the same as was used to test receiver components during fabrication.

After the system was tested up to its design operating temperature, the piping, tank, pump, and valves were insulated by the same contractor that insulated Sandia's portion of the system. The insulation used was the same type and was installed to the same specifications. In general, it consisted of several wraps or layers of fiberglass covered with aluminum sheet to hold it in place and prevent moisture from getting into it.

The downcomers were covered with special aluminum bellows flexible tubing. The insulation was segmented at the strainer and valves for cleaning and maintenance.

Portions of the control system were installed early so as to permit manual operation of the collector. However, because some wiring errors were made during the installation, some of the integrated circuit units failed. These failures made it difficult to bring the system to automatic control. However, when all the errors were corrected and the failed parts replaced, the control system performed as designed.

3. PRELIMINARY OPERATION

3.1. SYSTEM STARTUP

Actual system startup was performed in steps. The first operational test was to check out the drive system. The second step was to operate the fluid system and perform the safety pressure test. After these were accomplished, the system could be operated manually. The fluid flow rate could be regulated and the receiver could be brought into focus. Since the north row was ready for operation before the south row, it was operated separately, first making use of the bypass oil line. The operation of the north row permitted checkout of the control system. When the south row was completed and tested, the entire system was operated and pressure tested.

Prior to the safety pressure test, the system was heated up to and stabilized at 149°C (300°F) outlet oil temperature. The next step was to stabilize the outlet oil temperature at 177°C (350°F). Particular attention was given to the expansion of the receiver heat pipe as the system was progressively heated up. The receiver outlet was heated to 232°C (450°F) for the pressure test. The pressure source was hooked into the system, the oil heated up, and the receiver was defocused and the buffer tank valved out; then the pressure was raised in steps to 1380 kPa (200 psig). As previously noted, the pressure test was successful.

During startup, the oil was circulated internally through the buffer tank. This allowed the inlet temperature to rise nearly to the outlet temperature. This procedure checked the south row (and the whole receiver) at close to the operating outlet temperature.

The startup was hampered by a number of equipment problems and by cloudy weather. Finally, on June 26, 1978, electricity was generated with oil delivered from the FMSC subsystem to the Sandia storage tank.

3.2. EQUIPMENT MODIFICATIONS

During installation and startup, a number of equipment problems became evident. Those problems that were observed, corrected, or compensated for are enumerated here. The listing given below is approximately in the time sequence of occurrence or observation.

1. The pivot bolt coupling the radial arm and the jack extension tube together was made to the o.d. of the sleeve bearing in which the pivot bolt was to run. The design called for a shoulder bolt so that the nut could be tightened against a lock washer. The error required remachining to the proper diameter, i.e., to the i.d. of the sleeve bearing. The error was made by the vendor, who misinterpreted the drawing, and it slipped by the inspector. It was discovered at the time of installation.

   The solution was to use a standard bolt and double nut lock, which should have been used initially. The standard bolt worked well and no subsequent problems were observed. The bolt removes easily for receiver alignment and for changing the summer and winter brackets.

2. The jack mounting bracket, which also provided the mounting for the end pillow block support for the outer drive line, did not fit into the jack support base plate. There were two of these units for each row for a total of four units. The units had been made according to the fabrication drawing which, it was determined, did not show a cutout in the base plate for the bracket. The error was corrected in the field by making the required cutout using an oxy-acetylene torch, which was the only economical method available. However, the cutout edges were very rough as a result.

   The units were assembled, and the receiver rotation was checked out by driving it back and forth at least three times through its

total arc of travel. The assemblage was inspected carefully for possible binding that would impair the jack's motion. During these tests, the receiver drive operated as designed without any apparent malfunctioning. However, later the third jack screw from the west end of the north row snapped off at the collar. As a result, the receiver dropped causing severe leaks in the adjacent Marman clamp joints. The receivers, however, did not separate. A forklift was used to pick up the receiver and support it while repairs were made.

A spare jack was installed in place of the broken one. New gaskets were put into the Marman clamps. The thermal expansion loop joint (which was the joint where the jack broke) was not damaged. The keyed support shafts supporting the two receivers that fell were also replaced. The receiver was leak-tested to 414 kPa (60 psig) with dry nitrogen, and the repaired joints showed no leaks. Subsequent operation at the operating temperature showed some oil seepage out of one of the Marman clamps. Tightening the clamp stopped the seepage.

Investigating the cause of the failure revealed that a burr on the cutout edge on the jack-pillow block mounting bracket had caught on the edge of the support bracket of the jack mounting base plate. As a result, all four of the jack-pillow block mounting brackets were removed and sent to the shop to clean up the cutout edges. Also, when they were reinstalled, the tubular spacers were replaced with large, flat washers. No further trouble has been experienced in over a year of operation. This failure provided the first incident report for the FMSC subsystem. A copy of this incident report is included in Appendix B.

3. The primary speed reducer installed on the south row failed after a brief running period. Investigation showed that it had not been lubricated. The steel worm had worn off the teeth on the bronze

worm gear. The factory replaced the unit, which was then checked for lubrication. The unit installed on the north row was properly lubricated.

4. When the outlet oil temperature reached 232°C (450°F) the pipe on the north row had expanded sufficiently for the Marman clamp to catch the end support slide for the heat pipe. It was observed that the clamp band was partially pushed off, and at 315°C (600°F) this clamp would very likely fail. The support slide, which was attached to the radial arm assembly, was removed to allow the pipe to grow without being obstructed. No other problems due to thermal expansion were observed up to 315°C (600°F) oil outlet temperature.

5. After some time of operation, it was observed that the radial arms were leaning to the east, toward the side the pivot bearing was bolted to. The leaning appeared to get worse with time. Inspection revealed that due to the leaning the receiver end plate could bind on the radial arm. The probability of a structural failure in a high wind also increased as the leaning became more severe.

   The correction made was to put guy cables on the receiver radial arms to form a triangular brace that could be adjusted by turnbuckles. Initially six cables, three in each direction, were installed on each row. This method straightened the radial arms so they were perpendicular to the mirror axis. However, as the equinox was approached and the summer bracket had to be installed, these guy cables interfered with the receiver guide rod. It was then determined that only two guy cables were needed on each row, and they could be installed on the same receiver section. The one interfering guide rod in this section was removed.

6. After the summer bracket was installed and the receiver was lowered down to the horizontal, it was observed that the receiver deflection or sag between the supporting radial arms was excessive. The

design (and acceptable) deflection in this position was 0.95 to 1.27 cm (3/8 to 1/2 in.), but it was measured to be 2.9 ± 0.6 cm (1-1/8 ± 1/4 in.). This considerably increased light spillage, and made it difficult to adjust the tracking system to accurately track the focal line. Stiffeners had been attached to the secondary concentrator members to reduce the deflection; however, measurments showed that these were not effective.

A cable truss was therefore installed on the side of the receiver facing down in order to straighten the receiver. Turnbuckles were put on each end of the cable to permit adjustment of the tension.

The tension was adjusted so that the receivers were determined to be straight using line-of-sight alignment and a taut string check. It is necessary to reduce the cable tension when the receiver is on the winter bracket and the receiver is in a different orientation. If the tension is not reduced, the receiver will be deflected in the opposite direction. This could be avoided by using a cable truss on both sides of the receiver.

7. The control system faced one serious problem in the fluid control circuit, namely a very long sensor response time in the pump speed control. The platinum resistance thermometers (RTDs) were inserted into the receiver end fitting at each end of each receiver. Because the RTD access fitting was too large for the RTD fitting, a pipe bushing adapter was required. Since these fittings were threaded pipe, they were to be seal-welded in to prevent leakage. At the same time, it was necessary to be able to easily remove the RTD for maintenance, calibration, etc. A second small thermal well was welded into the receiver end fitting to seal the pipe and allow the RTD to be easily removed. However, later it was determined that the time constant for this assembly was so long it caused the control response to lag the temperature transients.

The correction made was to remove the thermal well and install the RTD directly into the fluid in the receiver end fitting. In the meantime, a pipe thread sealant was found that would seal the pipe connection against leakage of the hot oil. This correction shortened the time constant and improved the control system's response to temperature transients.

8. The torque tubes were coupled to the jacks by means of a spider coupling that was to allow for some torque tube shrinkage. However, on very cold mornings it was observed that some of the couplings very nearly separated. It became clear then that with large enough temperature swings the drive line could separate unobserved and result in serious damage to the receiver. The thermal expansion of the torque tube is about 1 cm (3/8 in.) for a temperature rise of about 38°C (100°F).

   The correction made was to replace the spider couplings with a flange coupling. Ideally, a splined coupling with a long engagement would be the best correction, but nothing was found commercially available that met this need. Therefore, a set of flanges were made that would slide on the shafts permitting expansion and contraction. This coupling, however, made the connection rigid, which introduced high stress on the shaft. Although two shafts broke, one on the torque tube and one on the jack, it was determined that flaws in the shafts were the reason. None of the other shafts broke after some 6 months of operation with the flanges.

9. It was also observed after operating for a while that the rotational slack seemed to be excessive. For some time, no apparent reason could be found for this slack. One of the "walking" inspections revealed that the keys in the couplings were working out of some of the key slots. The key installed was too short and could work all the way out. Upon replacing the key, the key slot in the shaft was

measured and found to be 3.9 mm (5/32 in.) instead of 3.2 mm (1/8 in.) as specified. This error contributed to the rotational slack of the drive line and was additive from one coupling to the next.

The correction made was to replace the torque tube end shafts with new shafts having the correct key way. But the weld attaching the end plate to the shaft was of low penetration, and when they were installed the weld cracked and failed on some of them. A composite correction was then made by using a 100% penetration weld and placing a neoprene shim between the plate and the torque tube to relieve the stress induced by the sag in the tube. The keys were then resistance-welded into the slots to prevent them from working out.

10. On July 17, 1978, the third tracking jack from the west end of the south row failed. At the time of failure, the receiver was in a nearly horizontal position. As the receiver dropped at the failed jack, it sheared off the screws attaching the adjacent supporting pillow blocks to the radial arm, allowing the next receiver to fall, which then sheared off the next screws. The effect dominoed to each end, dropping the whole south row receiver to the ground. The jack failure was caused by a locking key working loose. This failure was reported in Incident No. 2. This incident report is Appendix C.

    The whole receiver attachment was modified on both rows. Another, larger, "dumbbell" shaft was installed along with larger pillow blocks. These were attached to the radial arm with much larger 1 cm (3/8 in.) cap screws. A bridge was also installed across each receiver joint to prevent the receiver from coming apart at the pipe joint if a jack should fail. The subsystem was down until about mid-November 1978 while the repairs and modifications were made.

11. During August 1978, a severe hailstorm occurred at the site of the FMSC collector subsystem. Hailstones up to 1.9 cm (3/4 in.) in

diameter were reported. The hail cracked a number of mirror strips on the FMSC. Out of a total of 4128 mirror strips, some 400 were severely cracked in places and an additional 1500 suffered lesser damage.

Careful examination indicated that the broken mirrors had voids under them at the break point. All the severely broken mirrors examined had come loose from their bonding where they were broken. Other mirrors adjacent to those severely broken did not break if they were solidly bonded to the facet. This experience indicates that if a glass mirror is solidly bonded to a completely flat concrete facet, it will survive hail up to 3/4 in. in diameter. At this writing, the broken mirrors have not been removed or replaced.

The bonding agent used, 3M's Type 468, bonds the mirrors very tightly to clean concrete. However, it has since been discovered that if the concrete is not properly sealed, it forms a surface powder. This and any other surface dust either prevents the adhesive from sticking or allows it to come loose later. Most of the broken mirrors lie in the central part of each module near the tangent facet where the facet edges had broken (when the form was removed) and had later been repaired. These facets were dusty from honing down the repair. Water and compressed air were used to clean the facets prior to bonding down the mirrors, but they were not resealed. It has since been determined that this cleaning method is inadequate. Good bonding has been achieved by washing the slacking or dusty concrete with a muriatic acid solution and resealing. Breaking the sealant with abrasion or honing prevents adhesion, so if such repair methods are necessary an acid wash and resealing are needed to complete the repair.

3.3. SYSTEM PERFORMANCE

Initially, the FMSC subsystem was tested by delivering its oil to Sandia's blending tank. In this manner, the collector could be operated

under design conditions with the proper inlet and outlet oil temperatures. This also permitted operating the collector with lower than design oil outlet temperatures so that test data could be obtained at different temperatures. When these tests were completed and testing began at the design outlet oil temperature, oil was received from Sandia's cold oil storage [245°C (473°F)] tank and returned to Sandia's hot oil storage [310°C (592°F)] tank.

The data were acquired through Sandia's computer data acquisition system. Data were printed out at desired intervals, which usually were 1 to 5 minutes. In addition to the sensor data, certain calculated quantities such as the efficiency and the amount of heat delivered were also printed out. Each block of data printed included the following information:

1. The date
2. Solar time
3. Five front face pipe surface thermocouple temperatures
4. Two flow meters for main system oil flow
5. Normal incident pyroheliometer indication, W/m^2
6. Ambient air temperature
7. Wind speed and direction
8. FMSC subsystem temperature in, out, and ΔT
9. FMSC subsystem flow rate
10. Bulkhead temperature in, out, and ΔT
11. Heat gain in kilowatts
12. Efficiency
13. Integrated heat in kWh delivered to Sandia

In addition, the integrated solar insolation was available from a separate printout.

Copies of the printed data were obtained by GA from Sandia for the initial operation and, subsequently, for typical operating days. Not all the data availabe to date were obtained, but data from every test are available in the central computer file. The data from the specific tests and

times were tabulated and averaged. These sets of data were independently evaluated and compared with the printed data. Excellent agreement was obtained between the efficiency calculated from the data and the printed efficiency.

3.3.1. Thermal Efficiency

The efficiency was calculated by first averaging the inlet and outlet temperatures, the temperature rise, and flow rate over the period of time of interest. The Therminol properties were interpolated from the tables for the average Therminol temperature between the inlet and the outlet.

The heat out for the period of time of interest then is:

$$H_{out} = h_t \rho_t F \Delta T$$

where: h_t = Therminol heat capacity, Btu/lb-°F,

ρ_t = Therminol density, lb/gallon,

F = flow rate, gallons/minute,

ΔT = temperature rise, °F,

H_{out} = heat out, Btu/minute.

Also, for power:

$$P = \frac{H_{out}\ (Btu/min)}{3413\ Btu/kWh} \cdot \quad 60\ min/h = kW$$

The heat in is simply the pyroheliometer measurement times the collector area, i.e.,

$$H_{in} = IA \quad ,$$

where: I = insolation, kW/m^2,

A = collector area, m^2.

Then the efficiency is simply the ratio:

$$\eta = \frac{H_{out}}{H_{in}} \cdot \frac{60}{3413} = \frac{h_t \rho_t F \Delta T}{IA} \cdot \frac{60}{3413}$$

An overall summary of the performance is given in Table 3-1. The maximum solar noon efficiency acheived at operating temperature [outlet oil temperature at 315°C (600°F)] was 36.8% on December 5. This is substantially less than the peak of 42% that was measured at Sandia for the experimental test module.

Step increases in efficiency from one day to the following day can be noted in Table 3-1. These are due to cleaning the mirrors. The June 12 to 13, and June 19 to 20 runs, and some runs not reported here, show that about 5 percentage points in efficiency are gained right after a good mirror cleaning.

In this particular locale, the mirrors tend to get dirty quite rapidly and need to be cleaned frequently. Much of the area nearby is unpaved and two very busy streets are adjacent to the facility area. Experience shows that the wind blown dust washes off readily, but the deposit from auto exhausts causes a film that requires some mechanical scrubbing with detergent to remove. Sandia has reported that mild solutions of acetic acid will dissolve most of the film if it is not allowed to become too thick. In the facility area, the dust and film buildup occurs rapidly enough to significantly affect performance in about 2 weeks. Of course, this varies with the weather; it is much more rapid during windstorms.

Efficiency as a function of temperature is plotted in Fig. 3-1. The efficiency of the experimental module test unit is also shown for comparison. The effects of dirty mirrors and poor receiver alignment are indicated by the points below the line in Fig. 3-1.

Efficiency is plotted as a function of solar time in Fig. 3-2 for June 26, 1978, the first day electricity was produced from the FMSC collector subsystem. The peak efficiency reached on that day was 35.9%.

TABLE 3-1
SUMMARY OF FMSC PERFORMANCE DATA FOR
STABILIZED OPERATION CLOSE TO SOLAR NOON

Date	Solar Time		Temperature (°F)			Flow (gpm)	Insolation (W/m^2)	Average Peak Efficiency	kWh Produced	Integrated Efficiency
	From	To	Inlet	Outlet	ΔT					
May 9	11:39	12:04	242.5	372.2	129.7	11.84	1021.3	0.382	-	-
May 10	12:01	12:17	224.0	352.7	128.7	12.24	1020.0	0.382	-	-
June 6	11:43	12:33	317.6	452.4	134.9	9.133	967.0	0.344	-	-
June 8	11:46	12:27	302.5	499.7	147.2	8.854	972.1	0.363	-	-
June 12	11:54	12:29	366.5	501.9	135.4	8.436	947.7	0.334	49.43	0.321
June 13	11:39	12:24	363.0	503.0	140.0	8.766	904.6	0.379	66.53	0.359
June 14	11:42	12:45	314.0	494.4	180.4	6.868	939.5	0.364	90.07	0.340
June 15	11:43	12:27	436.4	550.7	114.3	10.541	986.9	0.345	66.96	0.332
June 16	11:37	12:25	416.6	557.2	140.6	9.328	1031.8	0.361	77.57	0.346
June 19	11:26	12:29	469.1	582.0	113.0	6.117	796.4	0.251	54.12	0.244
June 20	11:43	12:13	465.8	597.8	132.0	8.657	981.9	0.327	43.61	0.321
June 21	11:31	12:24	444.7	600.6	155.9	7.341	984.9	0.335	75.82	0.307
Nov. 17	11:49	12:22	474.1	602.5	128.4	9.637	1026.0	0.348	49.38	0.337
Dec. 5	11:37	12:11	450.9	607.6	156.7	8.300	1021.9	0.368	58.94	0.352
Dec. 12	11:48	11:58	486.0	617.8	131.8	9.440	1014.2	0.357	19.88	0.341
Dec. 12	12:20	12:27	484.9	605.9	121.0	10.634	1020.8	0.364	13.31	0.349
Dec. 21	11:44	12:22	451.7	596.4	144.7	6.880	1020.1	0.281	46.23	0.268
Jan. 20	12:26	13:14	467.8	600.6	132.8	6.528	1020.4	0.242	55.28	0.238

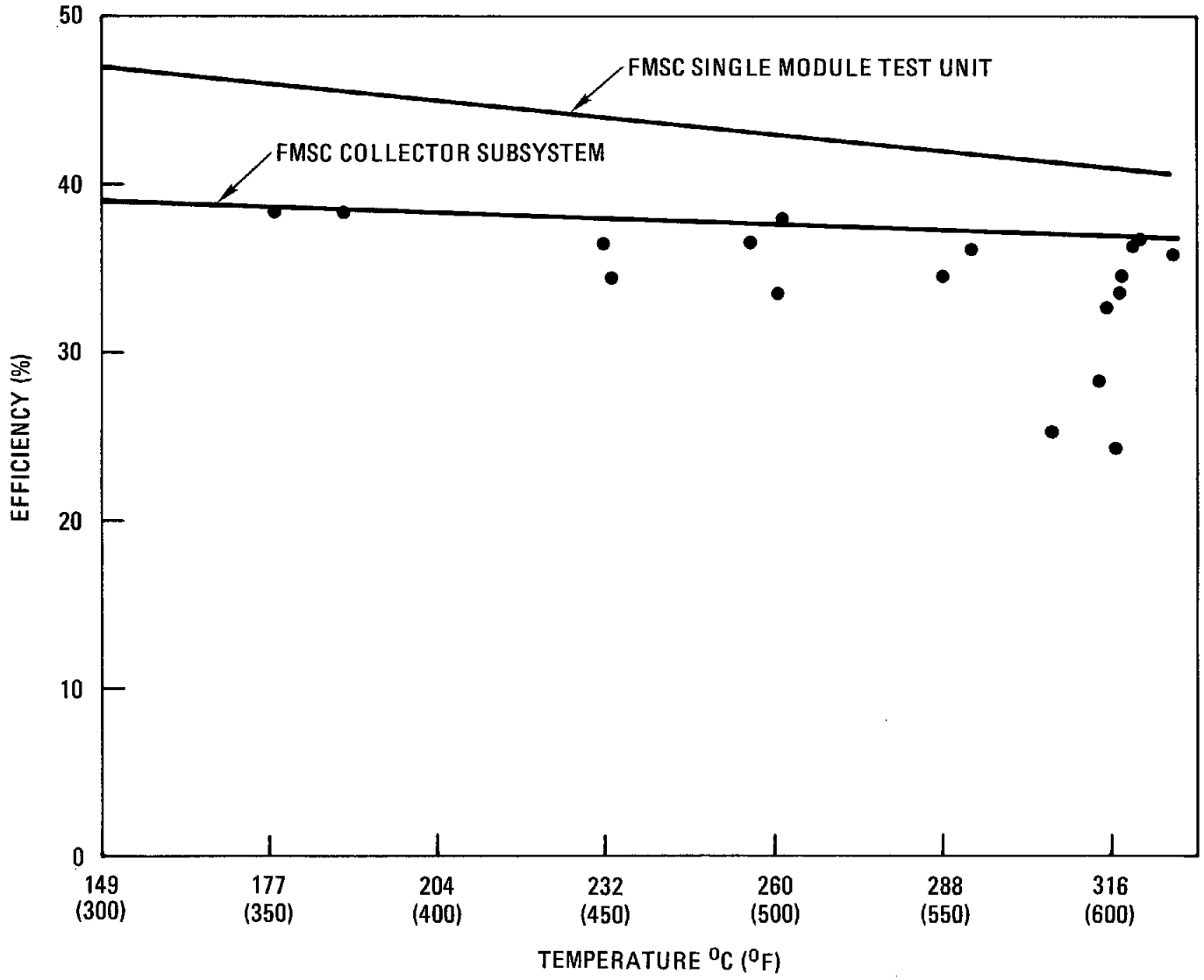

Fig. 3-1. Efficiency as a function of the outlet oil temperature comparing the performance of the test unit with the subsystem

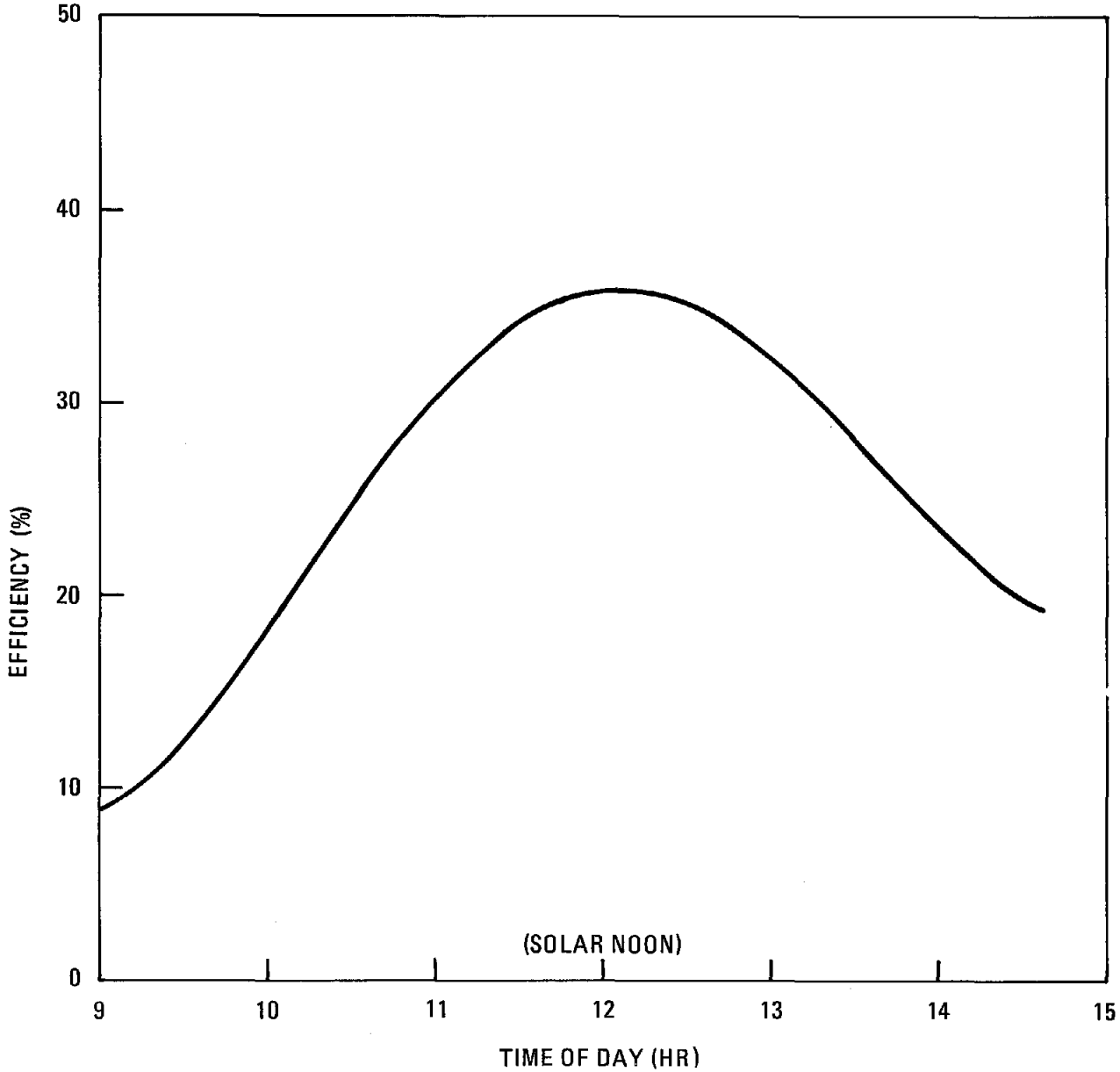

Fig. 3-2. FMSC collector subsystem efficiency curve for June 26, 1978 - the first day electricity was produced from the FMSC. Peak efficiency is 35.9%

3.3.2. Receiver Heat Loss

Two measurements were made of the heat loss between the inlet and outlet measurement points. One was made at an average fluid temperature of 166°C (332°F), and the other was made at an average fluid temperature of 204°C (399°F). The first measurement gave a total heat loss of 12.67 kW, which is equal to 48.7 W/m^2 of concentrator aperture. The second measurement gave a total heat loss of 18.54 kW, which is equal to a 71.3 W/m^2 aperture. This compares to 42.2 W/m^2 and 59 W/m^2 at the respective temperatures for the experimental test unit. The data are summarized in Table 3-2 and plotted in Fig. 3-3, which also shows the heat loss curve for the experimental test module.

The heat loss of the collector subsystem is considerably higher than for the experimental unit. This is due primarily to the following reasons:

1. The subsystem has at least 7.2 m (22.3 ft) of extra, nonheated pipe comprising the crossover pipe and flexible hose downcomers. It also has six thermal expansion loops, which amount to about 5.8 m (18 ft) of nonheated pipe. These pipes cause significant losses; they collect no heat but are included between the measurement points.

2. The insulation on the back of the subsystem heat pipe was only 1.59 cm (5/8 in.) thick, while it was 3.2 cm (1-1/4 in.) thick on the experimental unit.

3. The receiver heat pipe cross section is 2.5 cm (1 in.) x 6.35 cm (2.5 in.), while on the test unit the cross section was about 1 cm (3/8 in.) x 5 cm (2 in.). The larger exposed surface area, in particular, permits greater radiation and convective losses.

The data used for the second point for the subsystem in Table 3-2, obtained on June 14, 1978, are as follows.

TABLE 3-2
SUMMARY OF HEAT LOSS MEASUREMENTS ON THE FMSC COLLECTOR SUBSYSTEM COMPARED TO THE HEAT LOSS ON THE EXPERIMENTAL TEST UNIT

T_{in} (°C/°F)	T_{out} (°C/°F)	T_{AV} (°C/°F)	ΔT (°C/°F)	Heat Loss (kW)	Heat Loss Per Unit Receiver Length (W/m)[a]	Heat Loss Per Unit Aperture Area (W/m^2)	Notes
162/ 323	171/ 340	166/ 332	9/ 17	12.67	98.5	48.7	
198/ 388	210/ 410	204/ 399	12/ 22	18.54	144.1	71.3	93.35 w/m^2[b]
			Experimental Test Unit Heat Loss				
162/ 323	163/ 325	-	~1/2		45	42.2	
198/ 388	199/ 390	-	~1/2		63	59.0	

[a] Includes 7.2 m (22.3 ft) of crossover pipe and downcomers

[b] With ΔT measured at the bulkhead thermocouples

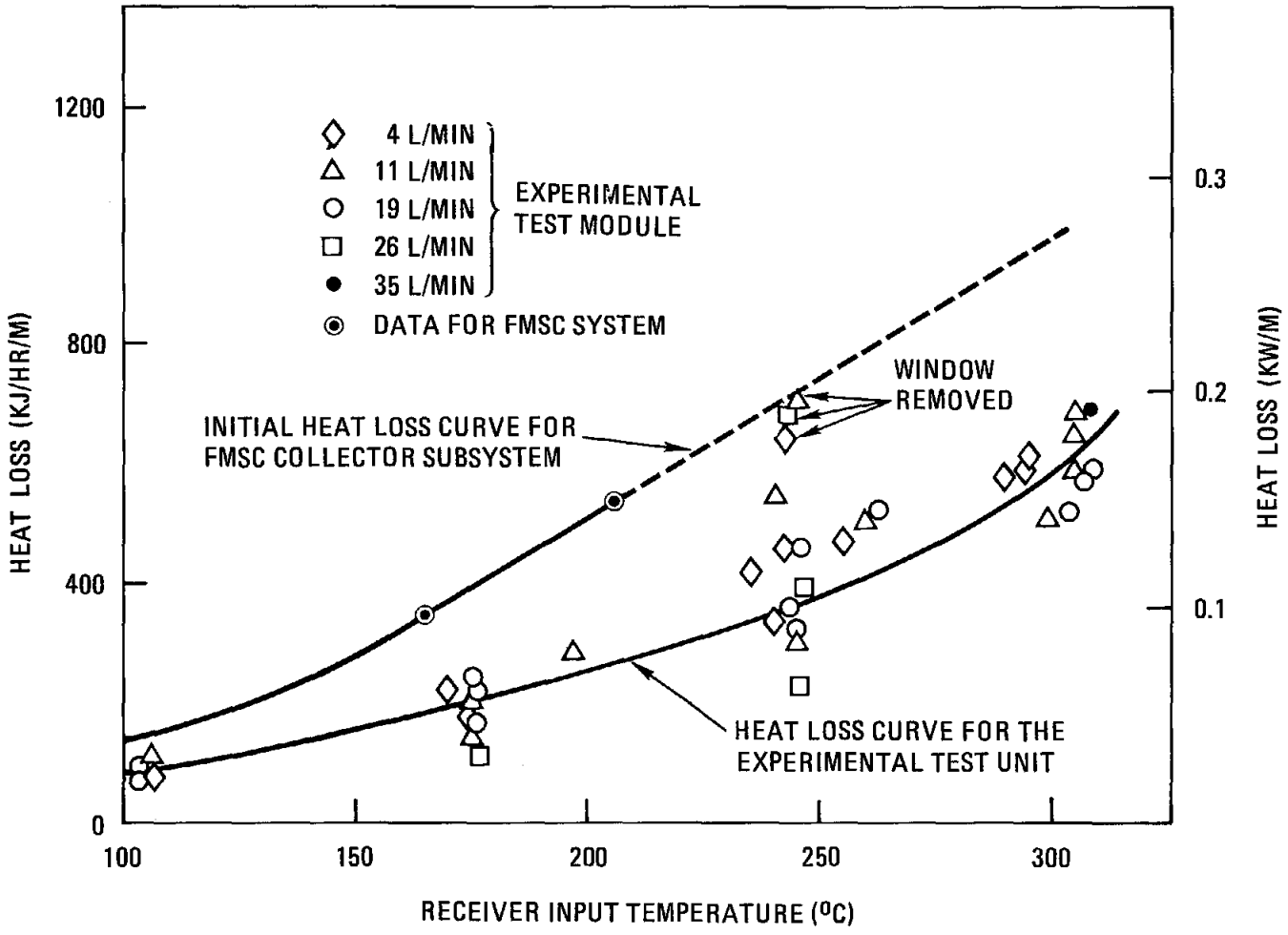

Fig. 3-3. Heat loss curve for the FMSC experimental test unit with the projected heat loss curve based on initial data

Solar time	9:47 a.m. to 10:30 a.m.
Average T_{in}, °F	410
Average T_{out}, °F	388
Average ΔT, °F	-22 (i.e., inlet higher than outlet)
Flow rate, gpm	12.214
Average ΔT at bulkhead, °F	-28.8
Average loss rate fraction	-0.087
Therminol heat capacity at 400°F	0.534 Btu/lb-°F
Therminol density at 400°F	7.35 lb/gal

The heat loss calculated from these data is

$$H_{loss} = 0.534 \frac{Btu}{16°F} \times 7.35 \frac{lb}{gal} \times 12.214 \frac{gal}{min} \times 22°F = 1054.7 \frac{Btu}{min},$$

$$= 144.1 \text{ W/m receiver plus crossover pipe,}$$

$$= 71.3 \text{ W/m}^2 \text{ aperture,}$$

at the average receiver temperature of 204°C (399°F).

If one uses the ΔT at the bulkhead, the total system heat loss including the pumps and buffer tank can be calculated. The resulting loss obtained is:

$$H_{loss \text{ bulkhead}} = 1380.6 \text{ Btu/min,}$$

$$= 24.271 \text{ kW,}$$

$$= 188.65 \text{ W/m}^2 \text{ receiver + crossover pipe,}$$

$$= 93.35 \text{ W/m}^2 \text{ aperture.}$$

Extrapolating the curve in Fig. 3-3 linearly to 311°C fluid outlet temperature indicates a heat loss of at least 275 W/m at operating conditions. This is equal to a total loss for the receiver and crossover pipe of 35.2 kW. For a very good solar day with insolation of 1020 W/m^2, this is a 13.2% loss.

3.3.3. Heat Pipe Skin Temperatures

The five sets of thermocouples on the heat pipe were located as follows:

1. Second receiver from inlet on the south row, about 8.5 m (28 ft) from the inlet thermowell.

2. Second receiver from the outlet of the south row, about 54 m (177 ft) from the inlet.

3. Second receiver from the inlet to the north row, about 76.2 m (250 ft) from the inlet.

4. Fourth receiver from the outlet, about 99 m (325 ft) from the inlet.

5. Second receiver from the outlet, about 6.7 m (22 ft) from the outlet or 122 m (400 ft) from the inlet.

Each set of thermocouples consisted of one iron-constantan and one copper-constantan thermocouple on the exposed or hot face of the heat pipe, and the same type pair on the back side of the heat pipe. The copper-constantan thermocouple on the hot face was used for over-temperature control. The remaining thermocouples were used for data, and their signals could be printed out. A summary of this data is given in Table 3-3. It is noted that the No. 5 thermocouples used for data sometimes indicate a negative ΔT between the front face (exposed to sunlight) and the back face. This says that the exposed face was at a lower temperature than the back face, which is not possible. Therefore, there is some malfunction or incorrect connection. The two thermocouples could have been reversed so that the ΔT would show the back side temperature higher than the front side. The ΔT was about the same in magnitude but opposite in sign. A plot of the hot and cold side pipe temperature throughout the day is shown in Fig. 3-4. This shows the sign reversal of the ΔT between the front and back face occurring

TABLE 3-3
SUMMARY OF HEAT PIPE SKIN TEMPERATURES FOR EACH OF THE FIVE LOCATIONS AVERAGED OVER THE TIME INDICATED

Date of Run	Solar Time Measurement Taken		Location No. 1			Location No. 2			Location No. 3			Location No. 4			Location No. 5		
1978	From	To	Front	Back	ΔT	Front	Back	ΔT	Front	Back	ΔT	Front	Back	ΔT	Front	Back	ΔT
June 6	10:50	12:3	375	337	38	397	359	38	442	402	40	455	420	35	487	438	49
June 8	10:41	12:0	374	337	37	394	355	39	450	472	38	461	428	33	494	442	52
June 8	12:8	14:29	360	334	26	381	353	28	432	409	23	450	427	23	473	440	33
June 12	10:10	11:59	419	385	34	441	404	37	496	459	37	507	478	29	532	492	40
June 12	12:33	14:32	417	393	24	436	410	26	484	464	20	496	474	22	527	499	28
June 13	9:45	11:57	418	383	35	441	403	38	500	463	37	515	481	34	543	497	46
June 13	12:27	13:31	414	391	23	436	408	28	484	463	21	502	477	25	531	494	37
June 14	9:47	10:30	402	404	-2	401	400	1	393	395	-2	391.5	395	-3.5	379.2	393	-13.8
June 14	11:5	11:58	413	376	37	440	398	42	500	469	39	514	477	37	549	500	49
June 14	12:7	13:2	388	357	31	416	381	35	475	452	23	504	479	25	525	485	40
June 15	10:52	12:4	490	458	32	508	474	34	552	518	34	556	533	23	586	547	39
June 15	12:37	13:23	478	450	28	496	466	30	545	517	28	550	531	19	530	504	26
June 16	10:1	12:6	476	439	37	496	458	38	550	512	38	559	530	29	594	547	47
June 19	9:54	11:41	528	497	31	550	516	34	593	560	33	602	579	23	612	593	19
June 20	9:58	10:27	533	499	34	559	519	40	590	554	36	601	574	27	594	581	13
June 20	10:36	11:27	517	483	34	541	503	38	600	562	38	608	581	27	598	566	32
June 20	11:35	12:9	527	493	34	545	509	36	597	562	35	600	578	22	592	563	29
June 20	12:52	13:15	517	490	27	536	506	30	587	560	27	589	574	15	587	555	32

TABLE 3-3 (Continued)

Date of Run	Solar Time Measurement Taken		Location No. 1			Location No. 2			Location No. 3			Location No. 4			Location No. 5		
1978	From	To	Front	Back	ΔT	Front	Back	ΔT	Front	Back	ΔT	Front	Back	ΔT	Front	Back	ΔT
June 21	9:57	12:12	517	485	32	539	504	35	596	562	34	600	578	22	615	593	22 [a]
June 21	12:19	14:50	508	484	24	529	502	27	585	560	25	590	576	14	(a)	(a)	(a)
Dec 5	10:36	11:59	(b)	-	-	-	-	-	594	561	33	617	592	35	621	590	31
Dec 5	12:3	14:41	(b)	-	-	-	-	-	591	565	26	607	582	25	615	592	23
Dec 12	11:44	12:14	(b)	-	-	-	-	-	607	577	30	620	594	26	629	598	31 [c]
Dec 12	12:21	12:27	(b)	-	-	-	-	-	590	575	15	606	590	16	620	600	20
Dec 12	12:45	13:10	(b)	-	-	-	-	-	590	566	24	608	584	24	620	594	26
Dec 21	10:53	11:59	(b)	-	-	-	-	-	588	559	29	617	585	32	607	587	20
Dec 21	12:3	14:30	(b)	-	-	-	-	-	593	566	27	609	585	24	614	597	17

[a] No. 5 TCs showed Neg ΔT's; i.e., back temperature was higher than front.

[b] No back face data since south row receiver repair because back face TC's were torn off.

[c] Same as (a) for this time segment.

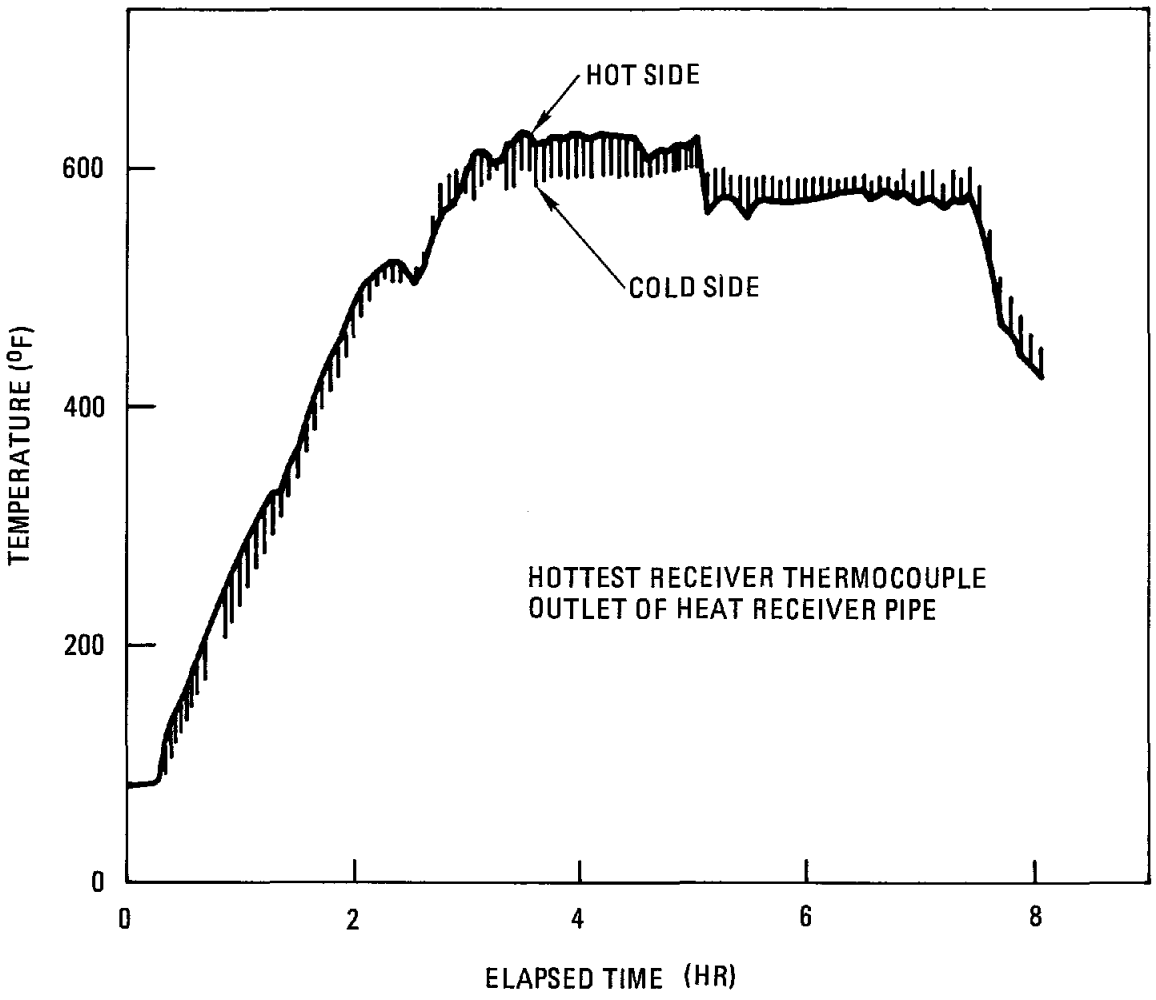

Fig. 3-4. Front and back temperature of the heat pipe as a function of elapsed time for the hottest (outlet end) pipe skin thermocouples. Note the reversal of ΔT polarity after noon

about noon. This sign change occurred on only a few days, and was recorded properly at other times as shown in Fig. 3-5 and Table 3-3. Figures 3-4 and 3-5 are for one day's run of the No. 5 location near the outlet. The ΔT for the other four locations and for a number of other data runs are given in Table 3-3.

There is considerable variation in the front face temperature compared to the back face temperature. This is due primarily to how well the peak light intensity is positioned on the thermocouples. The thermocouples are located on the center of the pipe, but because of poor receiver alignment, or because the receiver is tracking off from photocells on a different receiver, the maximum light intensity may not be positioned right on the thermocouples. However, as the receiver tracks, the peak intensity may traverse across the thermocouples. This results in variation of the front face thermocouple signal. The focal line generally does not have a flat intensity distribution at the top, but is very peaked as shown in Fig. 3-6, which gives plots of the light intensity across the focal line. The light intensity distribution varies throughout the day because the light source changes over four mirror segments and over two modules.

3.3.4. Fluid Temperature Control

The fluid temperature control system was installed, initially adjusted, and then operated. It did not control the outlet fluid temperature as well as was desired. Figure 3-7 is a plot of the outlet fluid temperature throughout the day on June 26, 1978, which is the first day the FMSC collector subsystem produced electricity. As shown in the plot, some instability occurred when the operating temperature was reached. Also, the temperature tended to drift away from the demand set point. Several problems (previously discussed) were found and solved. In July, the control system was to be optimally adjusted, but the receiver failure occurred, preventing completion of the fluid control adjustment.

In January 1979, after the receiver was repaired and the system operated, the final adjustments were made. Figure 3-8, a plot of the fluid

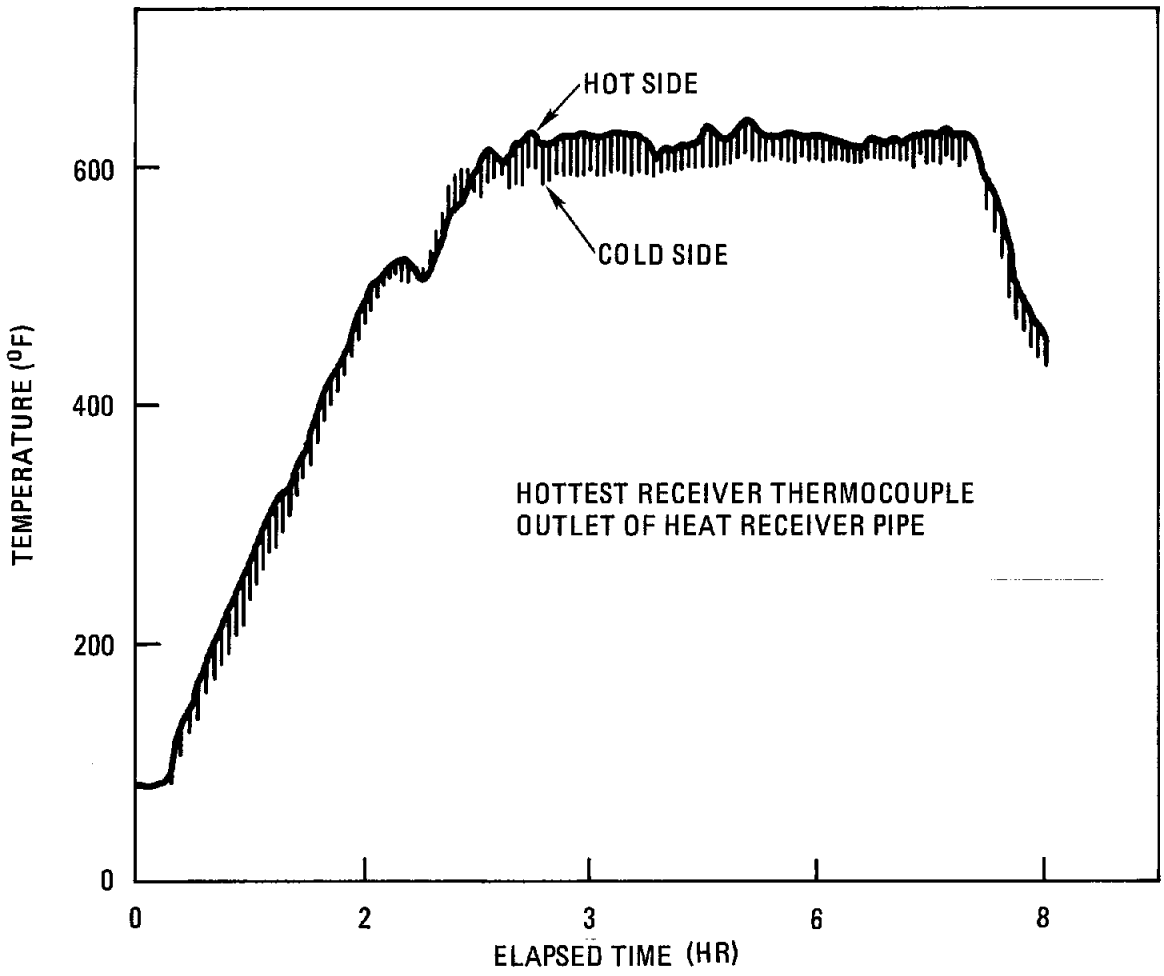

Fig. 3-5. Front and back temperature of the heat pipe as a function of elapsed time for the hottest (outlet end) pipe skin thermocouples

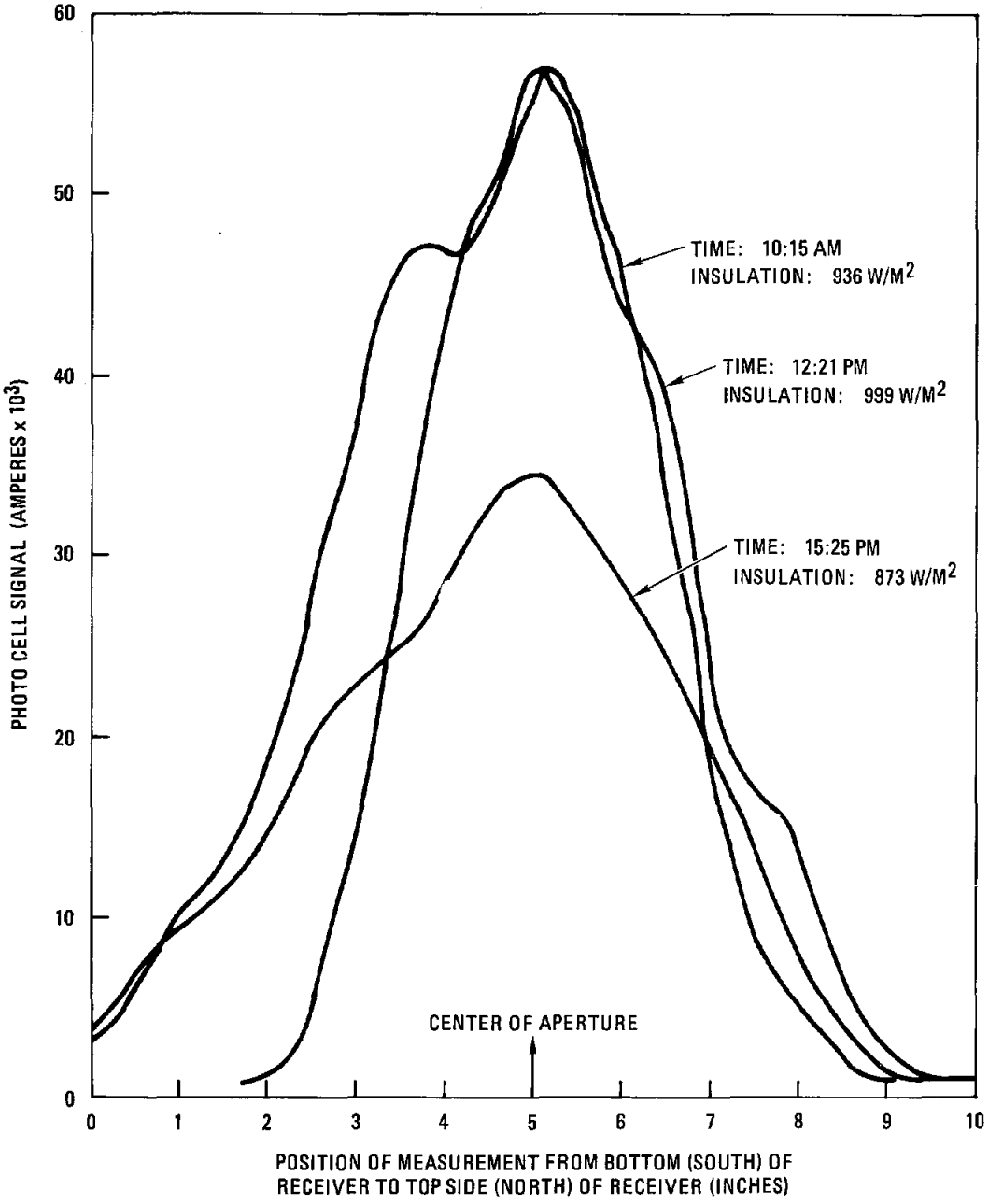

Fig. 3-6. Position of measurement from bottom (south) of receiver to top side (north) of receiver. Height intensity distribution across receiver aperture for three different times

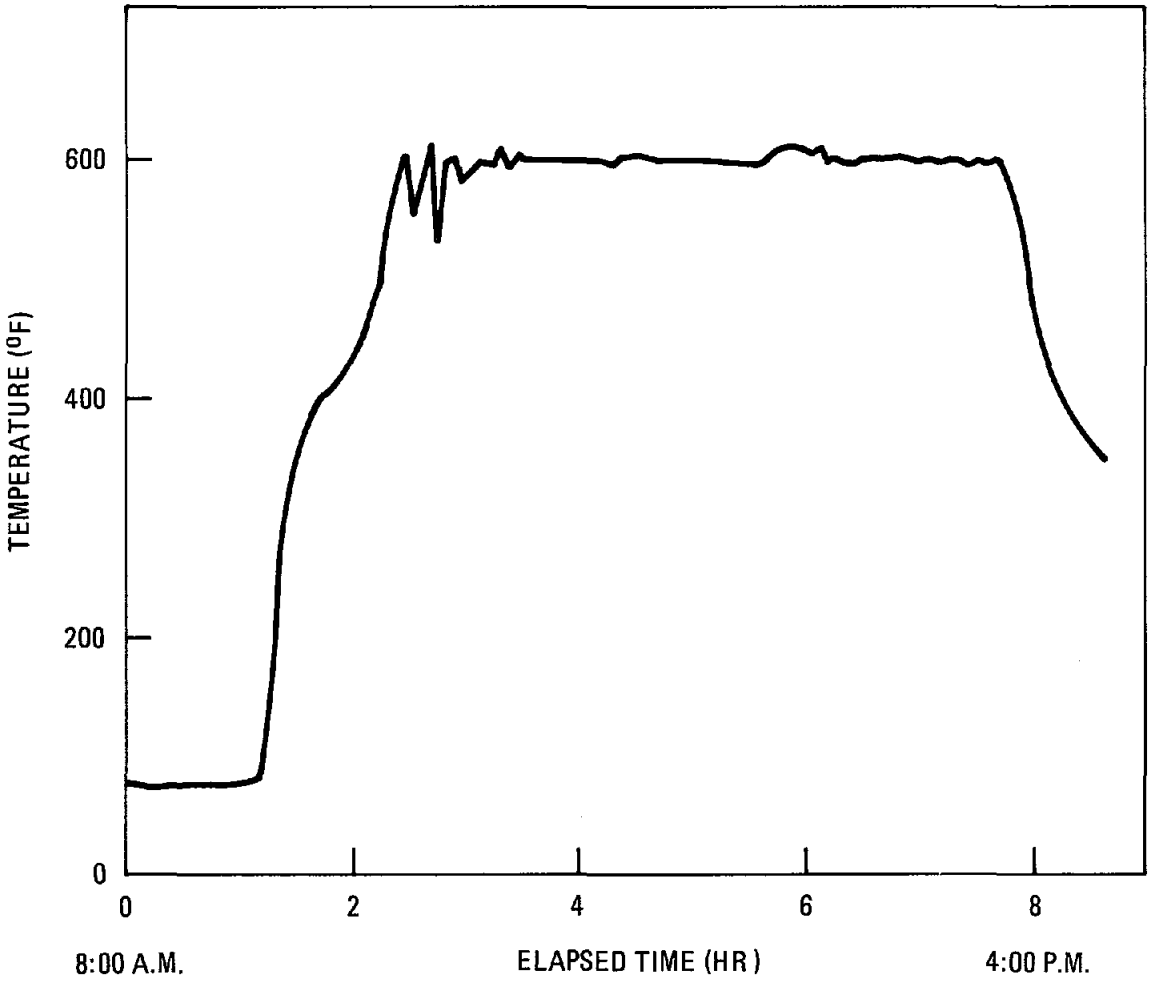

Fig. 3-7. Outlet oil temperature as a function of elapsed time on the June 26 test - the first time electricity was produced from the FMSC

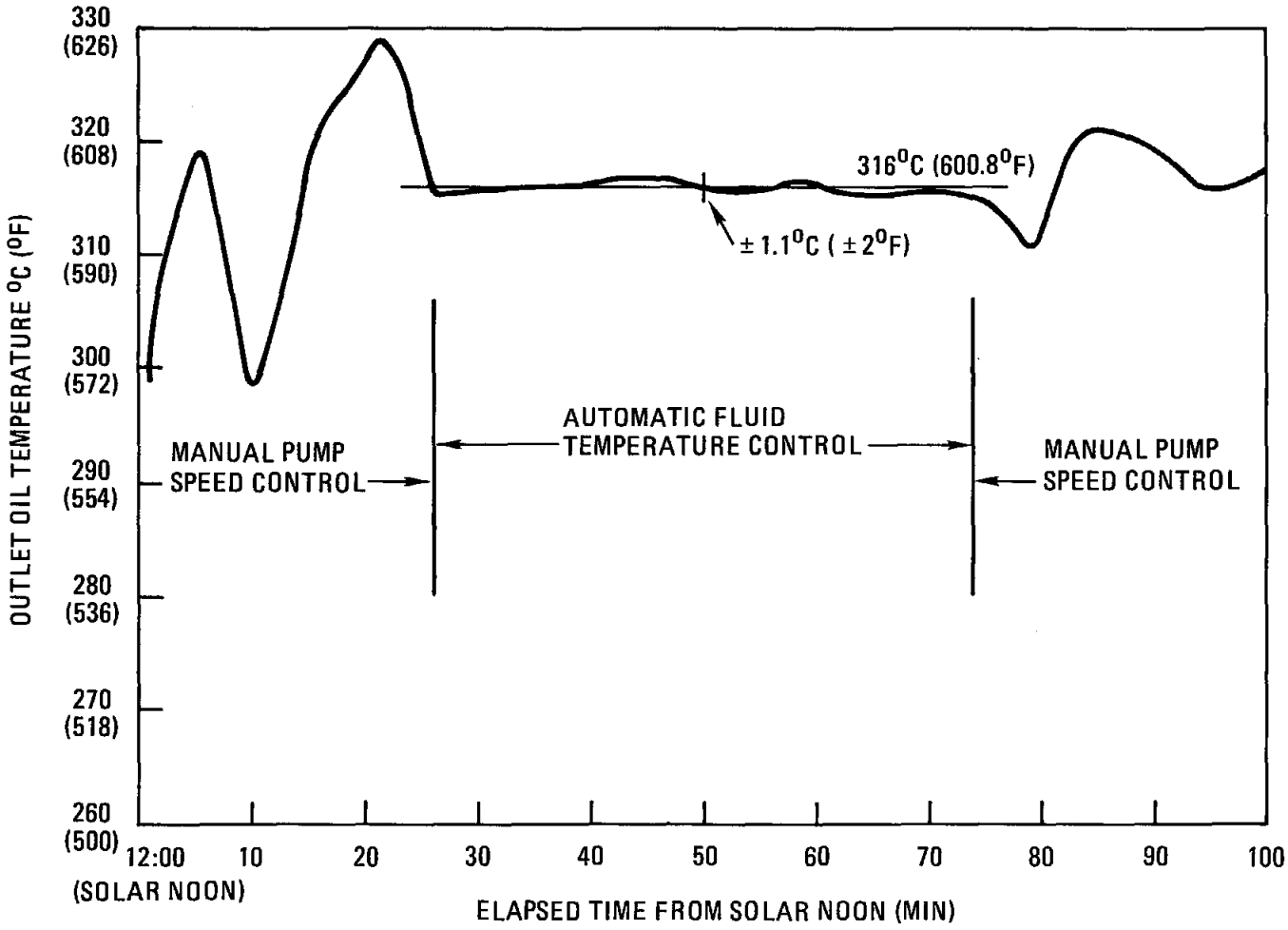

Fig. 3-8. Outlet fluid temperature versus time after adjustment and calibration of automatic fluid outlet temperature control

outlet temperature as a function of elapsed time, shows that the fluid outlet temperature is being controlled to 316°C ± 1.1°C (600.8°F ± 2°F). Additional testing was attempted, but bad weather prevented successful test completion. The temperature control was set to regulate the outlet oil temperature to 316°C (600.8°F) so that the oil delivered to Sandia's hot storage tank would be 311°C ± 2°C (592°F ± 5°F). The control system, therefore, controls the oil temperature well within the required bracket.

3.3.5. Performance Analysis

The performance of the subsystem is lower than that calculated. A summary of expected and actual performance is listed below:

Calculated efficiency, equinoxes	0.50
Calculated efficiency, solstices	0.46
Best obtained, December 5	0.368

A series of measurements were made on the experimental test module to quantify the receiver light spillage, i.e., the receiver capture fraction. These measurements were made by traversing a photocell across the focal line at the receiver aperture position. Three such traverses are shown in Fig. 3-6. Traverses were made at five different points along the mirror for each of five mirror segments. These data were evaluated and the results are given in Table 3-4. The average capture fraction determined by this method is 71.3% ± 8.4%.

Several checks were made on the FMSC subsystem receiver, and it was found that the individual receiver segments under measurement would perform better than this. It was also found that the receiver line (i.e., eight receiver units) was not straight, and neither was the focal line. This meant that a given receiver segment could perform significantly better than the whole receiver line performed. Correlating the thermal efficiency and heat loss data with the other system parameters indicates that the secondary concentrator (i.e., receiver) light capture fraction is about 0.734. Table 3-5 gives the data for the best thermal efficiency obtained at operating temperature.

TABLE 3-4
LIGHT COLLECTION EFFICIENCY MEASUREMENTS
FOR THE EXPERIMENTAL TEST MODULE

Position Mirror Segment No. From East End	Solar Time	Julian Day	ϕ[a]	$\frac{dC}{dP}$[b]	Δ[c]	$4.5\ \frac{0.125}{\Delta}$[d]	Light Collection Efficiency[e]
1	11:50	284	46°	3.9700	0.1764	3.188	63.0%
2	12:43	278	49°	4.2235	0.1877	3.000	79.1%
3	11:12	278	49°	4.2235	0.1877	3.000	81.5%
4	12:09	278	49°	4.2235	0.1877	3.100	65.6%
5	12:30	285	46°	3.9700	0.1764	3.188	67.3%

(a) ϕ = Component of sun's angle above the southern horizon.

(b) dC/dP = The rate of change of the receiver travel with respect to the ball nut travel, i.e., with respect to the drive shaft rotation.

(c) Δ = The actual data point spacing across the focal line.

(d) $4.5\ \frac{0.125}{\Delta}$ = Apparent apperture width compared to the actual secondary aperture of 4.5 in. with the nominal data spacing of 0.125 in.

(e) Average 71.3% ± 8.4%

TABLE 3-5
PERFORMANCE COMPARISON BETWEEN 260 m^2 FMSC FIELD
AND EXPERIMENTAL MODULE TEST UNIT

Optical Loss Factor	Value		Method of Determination
	Experimental Test Module	Subsystem Field	
Shadow	0.93	0.92	Measured
Primary mirror reflectivity	0.96	0.96	Measured
Glass thickness edge effects	0.96	0.96	Estimated
Secondary concentrator light capture fraction	0.71	0.734	Measured
Secondary concentrator reflectivity (0.85) corrected for fraction of light directly striking receiver tube	0.92	0.92	Measured
Transmission of window (0.95) corrected for angular dispersion	0.92	0.92	Measured
Receiver tube blackness	0.95	0.95	Measured
Overall optical efficiency	0.489	0.500	
Less thermal losses (at 311°C outlet temperature)	0.062	0.132	Measured
Net FMSC efficiency at operating temperature	0.427	0.368	

There are several reasons why the light loss, due to spillage and window transmission loss. is this high. Some of these are enumerated below.

1. Precision and straightness of the focal line is less than should be achievable. Improving precision of the primary mirrors and module positioning would improve the focal line.

2. The alignment of the receiver itself, which can be adjusted to some degree, is not as good as should be achievable. Improving the receiver straightness and positioning will reduce spillage.

3. The receiver window tends to get dirty on the back side because of dust from the Microtherm insulation. Sealed insulation would prevent this.

A summary of the FMSC collector subsystem performance, presented in Fig. 3-9, was supplied by Sandia Laboratories. The effect of dirt on the mirrors is graphically shown in this figure. After 16 days without cleaning, the efficiency dropped about 6%. Straightening the receiver improved the efficiency about 1.5%. The difference, then, between dirty mirrors (after 16 days without cleaning) and the straightened receiver is about 7.5%. These data were taken in December 1978 using the hail-broken mirrors. Since the hail storm came shortly after the receiver failure, no direct measurement of the effect of the broken mirrors exists; however, it is estimated that the breakage produced another 2% loss.

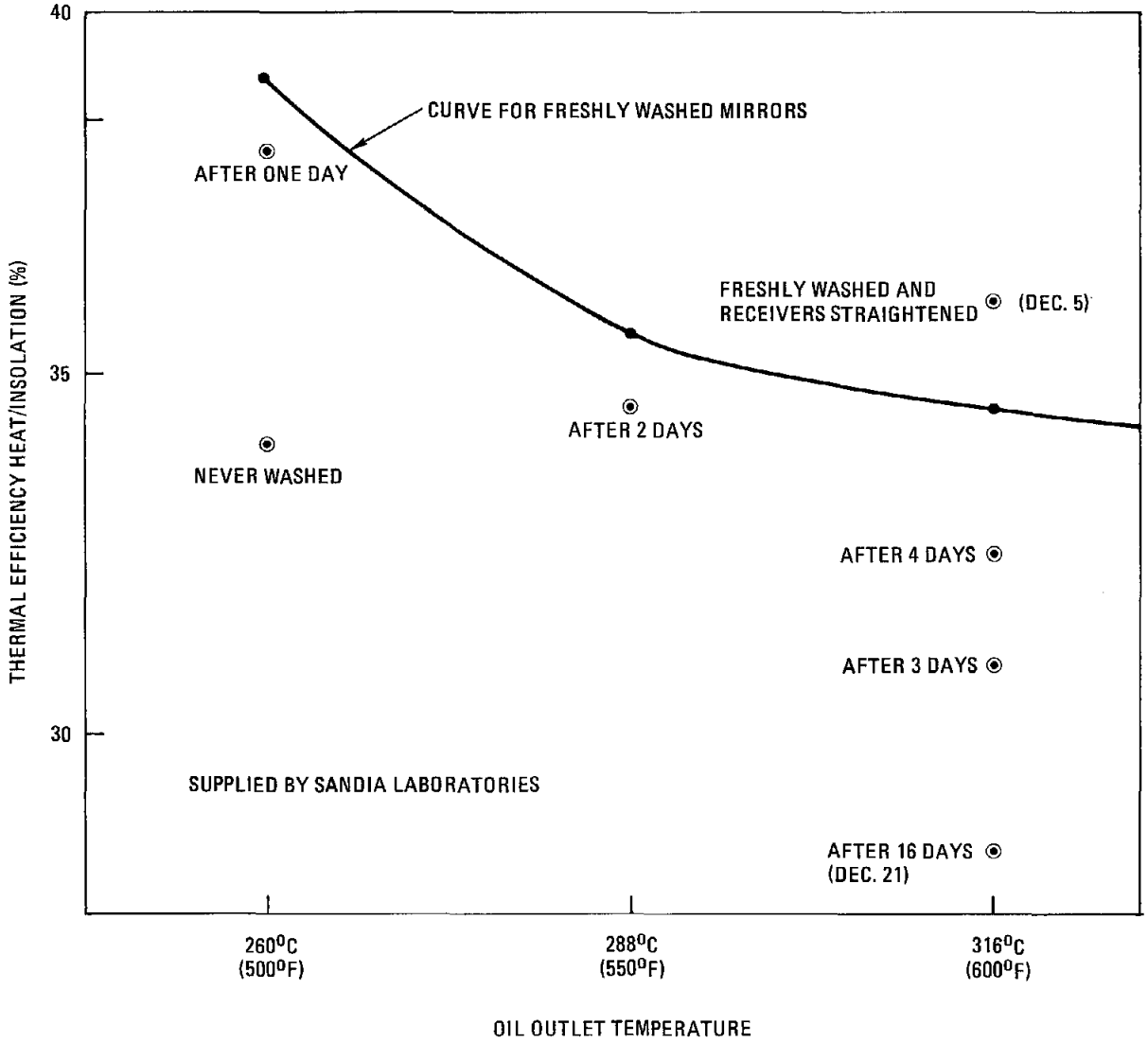

Fig. 3-9. Summary of the FMSC collector subsystem noontime efficiency corrected to 1000 W/m^2

4. COST ANALYSIS

The cost analysis section is divided into two parts. The first part addresses the actual cost of the subsystem, and the second part addresses the various possibilities for cost reduction and develops a projected commercial system cost.

4.1. SUBSYSTEM COST

The total cost of the subsystem can be conveniently divided into four categories:

1. Project management
2. Subsystem engineering
3. Components, hardware, and installation
4. Startup and preoperation testing

The project management cost consisted almost entirely of the project manager's work during the duration of the project. Since the project was too small to support a full-time project manager within a reasonable budget, the project manager participated heavily in the engineering function and the site construction work. This reduced the support that otherwise would have been required. As a result of this, the overall costs were reduced but the apparent management cost increased. On a large commercial project, the relative management costs would be much less.

The subsystem engineering costs are divided into three subcategories: (1) the subsystem engineering performed by GA, (2) the site engineering contracted to Allison Engineering Company and funded by Sandia, and (3) the foundation engineering contracted to Allison Engineering by Sandia Laboratories. The individual costs are listed in Table 4-1.

TABLE 4-1
MAJOR FUNCTION COST SUMMARY FOR THE
260 m^2 (2800 FT^2) FMSC COLLECTOR SUBSYSTEM

Function	Function Cost	Total Cost	Cost/ft^2
Management	64,909	64,909	23.18
Engineering, GA	98,764	-	-
Allison, GA Contract	5,463	-	-
Allison, Sandia Contract	4,000	-	-
Total Engineering	-	108,227	38.65
Preconstruction Testing	15,965	15,965	5.70
Module Form Fabrication	149,323	149,323	53.33
Subsystem Fabrication & Installation	201,136	201,136	71.84
Startup and Preoperating Testing	39,440	39,440	14.09
Total Cost		579,000	206.79
Equals			2225.06/m^2

The subsystem fabrication and installation costs are itemized in Table 4-2. These costs are a little below the true costs because support that Sandia gave the project is not included. There is no accurate way to show the effect of this support on the final cost of the collector subsystem, but GA acknowledges this support. Table 4-2 tabulates these subsystem costs to the lowest element that an individual item can be identified, and also shows its cost normalized per square foot of aperture area.

The startup and preoperation testing cost became higher than anticipated because of various new system startup problems. It would certainly seem that many of these costs would not be necessary on subsequent plants.

4.2. PROJECTED COMMERCIAL SYSTEM COST

This study was done in two steps. The first step was to develop the cost of a second plant (i.e., a demonstration model) which would incorporate the learning gained on the Sandia experimental model. The size of this demonstration unit for cost evaluation was 9290 m^2 (100,000 ft^2) of aperture. This size was large enough to incorporate some new production techniques, gain commercial pricing for components and supplies, and amortize tooling costs over a large enough area to significantly reduce their unit area cost. These costs for each item are listed in Table 4-3.

The second step assumed full commercial development, but did not assume any large changes in the basic design from that of the Sandia unit. Commercial development means here that manufacturing facilities have been built to use mass production techniques for component fabrication, assembly, and installation. To evaluate commercial costs, a production capability of 929,000 m^2 (10 million ft^2) per year was assumed. For this study a plant size of 92,900 m^2 (1 million ft^2) was assumed, which is not into the regime of large central station power but is a nominal projected size for an intermediate size plant for process heat and total energy applications as well as power generation. These costs for each item are listed in Table 4-4 and are summarized in Table 4-5. The costs are given in 1977 dollars, i.e., the year the Sandia FMSC subsystem was contracted for, and do not include any fee or profit allowances.

TABLE 4-2
COST ITEMIZATION OF THE 260 m^2 (2800 FT^2) FMSC COLLECTOR SUBSYSTEM AT SANDIA LABORATORIES

Component or Item	Unit	No. Required	Unit Cost	Total Cost	Cost/ ft^2
Primary Concentrator					
Mirror Glass	Sheet	-	-	1,880	0.67
Mirrors, Cut, Silvered, Coated	2 in x 50 in	4,128	1.95	8,050	2.87
Fiber Concrete for Modules	2.34 yd ea	32	208.25	6,664	2.38
Other Module Materials	Module	32	72.47	2,319	0.83
Labor - Module Casting	Module	32	295.13	9,444	3.37
Mirror Adhesive	Roll	96	10.97	1,053	0.38
Mirror Installation - Labor	Mirror	4,128	2.52	10,400	3.71
Sub-Total				39,810	14.22 = 153.01/m^2
Installation - Mirror Module					
Foundations	Ea	34	280.00	9,533	3.40
Equipment Rental	Hour	45	25.00	1,125	0.40
Module Alignment	Lot	-	-	2,264	0.81
Grout Bases	Lot	34	44.12	1,500	0.54
Oil Catch Sump	Ea	1	1,500.00	1,500	0.54
Utility Power	Lot	-	-	1,300	0.46
Utility Water	Lot	-	-	1,300	0.46
Paving and Pad	Lot	-	-	2,839	0.01
Sub-Total				21,361	7.63 = 82.10/m^2
Support Structure					
Tracking Motor	Ea	2	200.00	440	0.16
Tracking Motor Controller	Ea	2	281.00	562	0.20
Tracking Drives	Ea	18	313.78	5,648	2.02
Support Members	Set	18	454.11	8,174	2.92
Bearings	Set	18	88.33	1,590	0.57
Speed Reducer	Ea	2	100.00	200	0.07
Limit Switches	Ea	8	22.34	180	0.06
Control Potentiometer Assy	Ea	4	51.40	212	0.08
Summer Bracket	Ea	18	58.89	1,060	0.38
Painting	Lot	-	-	500	0.18
Installation	Lot	18	-	1,443	0.52
Alignment	Lot	18	-	5,565	1.99
Sub-Total				25,574	9.13 = 98.24/m^2

TABLE 4-2. (Continued)

Component or Item	Unit	No. Required	Unit Cost	Total Cost	Cost/ ft^2
Control System	Ea	1	20,850	20,850	7.45
Installation & Checkout	Lot	-	-	15,000	5.36
Electrical Wiring	Lot	-	-	5,500	1.96
Thermocouple Wire	Lot	3,000 ft	140/m	420	0.15
Emergency Power Source	Ea	1	2,100.00	2,100	0.75
CTU Pedestal	Ea	1	100.00	100	0.04
Sub-Total				43,970	15.70 = 168.93/m^2
Receiver					
Aluminum Channel	Ea	16	67.00	1,072	0.38
Secondary Con. Extrusions	Ea	32	77.13	2,468	0.88
King-slux	Ft	50	45.50	728	0.26
Rectangular Heat Pipe	Ft	25	46.06	737	0.26
Microtherm Insulation	Ft	25	307.19	4,915	1.76
Teflon Window	Ft	25	13.88	222	0.08
Heat Pipe Plating	Ea	16	117.50	1,880	0.67
Heat Pipe Welding, Adaptors	Ea	32	225.81	3,613	1.29
Stainless Steel Foil	Ft	25	49.38	790	0.28
Marnan Clamps	Ea	12	90.00	1,080	0.39
Marnan Clamp Seals	Ea	12	6.00	72	0.03
Flex Hose Adaptor Fittings	Ea	12	16.00	224	0.08
Flex Thermal Expansion Loops	Ea	6	142.00	852	0.30
Flex Hose Downcomers	Ea	4	381.75	1,527	0.55
End Connection Adaptors	Ea	4	183.75	735	0.26
Misc. - Covers, Brackets, etc	Lot	-	-	1,664	0.59
Receiver Assy	Lot	-	684.81	10,957	3.91
Sub-Total				33,436	11.94
Installation	Lot	16	300.00	4,800	1.71
Total				38,236	13.65 = 146.87/m^2

TABLE 4-2. (Continued)

Component or Item	Unit	No. Required	Unit Cost	Total Cost	Cost/ ft^2
Fluid System					
Pump	Ea	2	1,296.00	2,592	0.93
Motor	Ea	2	533.58	1,067	0.38
Motor Controller	Ea	2	316.14	632	0.23
Powered Oil Valves	Ea	3	428.50	1,285	0.46
Manual Valves	Ea	13	72.00	936	0.33
Strainer	Ea	1	131.00	131	0.05
Pressure Relief Valves	Ea	6	152.90	917	0.33
Buffer Tank	Ea	1	1,459.00	1,459	0.52
Powered Nitrogen Valves	Ea	3	364.10	1,092	0.39
Nitrogen Check Valves	Ea	2	30.60	61	0.02
Turbine Flow Meter + Gauge	Ea	1	1,220.00	1,220	0.44
Orifice Flow Meter + Gauge	Ea	1	365.00	365	0.13
Pressure Gauges	Ea	2	57.07	114	0.04
Pump Flex Connectors	Ea	6	42.16	253	0.09
Fluid Level Sensors	Ea	2	214.00	428	0.15
Air Solenoid Control Valves	Ea	6	38.50	231	0.08
Sub-Total				12,783	4.57 = 49.17/m^2
Pipewelding & Installation	Lot	-	-	10,394	3.71
Pipe Insulation	Lot	-	-	5,508	1.97
Bypass Line + Insulation	Lot	-	-	3,500	1.25
Sub-Total				19,402	6.93 = 74.57/m^2
Grand Total				201,136	71.83 = 772.89/m^2

TABLE 4-3
COST SUMMARY BY SYSTEM AND TASK OF THE
240 m^2 (2800 FT^2) FMSC COLLECTOR SUBSYSTEM

System or Task	Unit	No. Required	Unit Cost	Total Cost	Cost/ ft^2
Primary Concentrator	Module	32	1,244.00	38,810	14.22
Installation in Field	Module	32	667.53	21,361	7.63
Support Structure	Set	34	546.06	18,566	6.63
S.S. Installation	Set	34	206.12	7,008	2.50
Receiver Fabrication	Ea	16	2,089.75	33,436	11.94
Receiver Installation	Ea	16	300.00	4,800	1.71
Fluid System	Lot	-	-	12,783	4.57
F.S. Installation & Insulation	Lot	-	-	19,402	6.93
Control System	Lot	-	-	20,850	7.45
C.S. Installation & Checkout	Lot	-	-	23,120	8.26
Total				201,136	71.84 = 773.00/m^2

TABLE 4-4
ITEMIZED COST PROJECTION FOR THE NEXT
PLANT AND FOR A COMMERCIAL PLANT

Component or Item	Unit	Cost/ft^2 ($) Size or No. Required	Next Unit 100,000 ft^2	Size or No. Required	Cost/ft^2 Comm. Unit 10^6 ft^2
Primary Concentrator					
Mirror Glass	Sheet	Sheet	0.40	Prefab Strip	0.20
Mirrors, Silvered & Treated	Unit	3 in.x 75 in.	1.60	Cont. Strip	0.30
Fiber Concrete for Modules	Ea 300 ft^2	5.00 yd	1.40	300 ft^2	0.80
Other Module Materials	Module	∿330	0.60	3,340	0.30
Labor Module Casting	Module	∿330	2.50	3,340	1.00
Mirror Adhesive	Rolls	2,250	0.25	Prefab on Mirror	0.20
Mirror Installation	Mirror	64,680	1.25	646,800	0.60
Sub-Total			8.00		3.40
Installation - Mirror Module					
Foundations	Ea	∿350	2.25	Cont.	1.00
Equipment Rental	Day	12 days	0.05	80 days	0.03
Module Alignment	Lot	-	0.20	-	0.17
Grout Bases	Not Needed		-	-	-
Oil Catch Sump	Ea	10	0.15	100	0.10
Utility Power	Lot	-	0.10	-	0.05
Utility Water	Lot	-	0.10	-	0.05
Paving and Equip. Pads	Lot	-	0.50	-	0.20
Sub-Total			3.35		1.60
Support Structure					
Tracking Motors	Ea	40	0.08	400	0.06
Tracking Motor Controllers	Ea	40	0.10	400	0.08
Tracking Drives	Ea	360	1.08	3,600	0.70
Support Members	Set	360	1.90	3,600	1.00
Bearings	Set	Not Needed	-	-	-
Speed Reducers	Ea	40	0.03	400	0.02
Limit Switches	Ea	160	0.03	1,600	0.02
Control Potentiometers	Ea	80	0.03	800	0.02
Summer Bracket	Ea	Not Needed	-	-	-
Painting	Lot	-	0.08	-	0.04
Installation	Lot	-	0.37	-	0.26
Alignment	Lot	-	0.50	-	0.30
Sub-Total			4.20		2.50

TABLE 4-4. (Continued)

Component or Item	Unit	Cost/ft^2 ($) Size or No. Required	Next Unit 100,000 ft^2	Size or No. Required	Cost/ft^2 Comm. Unit 10^6 ft^2
Control System	Ea	1	0.50	M-S Sets	0.40
Installation & Checkout	Lot	-	0.30	-	0.30
Electrical Wiring	Lot	-	0.50	-	0.22
Thermocouple Wire	Lot	60,000 ft	0.10	600,000	0.08
Emergency Power Source	Ea	1/array	0.18	1/array	0.15
CTU Pedestal	Ea	1/array	0.01	1/array	0.005
Sub-Total			1.59		1.155
Receiver					
Aluminum Channel	Ea	∿330	0.22	∿3,300	0.20
Secondary Con. Extrusion	Ea	∿660	0.50	∿6,600	0.45
Secondary Reflector	Kinglux	16,000 ft	0.12	160,000 ft	0.10
Heat Pipe	Tube	8,000 ft	0.12	80,000 ft	0.10
Heat Pipe Insulation	Not Needed		-	-	-
Glass Tube	Ea	8,000 ft	0.32	80,000	0.25
Heat Pipe Plating	Per ft	8,000 ft	0.40	80,000	0.30
Heat Pipe Welding	Set	320	0.50	3,200	0.20
Stainless Steel Foil	Not Needed		-	-	-
Heat Pipe Fittings	Set	320	0.25	3,200	0.15
Thermal Expansion Joints	Set	320	0.32	3,200	0.24
Flexible Downcomers	Ea	80	0.31	800	0.20
End Connection Adaptors	Ea	80	0.15	800	0.10
Misc. Covers, Brackets, etc.	Lot	-	0.34	-	0.25
Receiver Assembly	Lot	-	1.50	-	0.50
Field Installation	Lot	-	0.50	-	0.30
Sub-Total			5.55		3.34
Fluid System					
Pump	Ea	10	0.13	24	0.06
Motor	Ea	10	0.05	24	0.025
Motor Controller	Ea	10	0.03	24	0.02
Powered Oil Valves	Ea	15	0.06	36	0.02
Manual Valves	Ea	30	0.03	72	0.01
Buffer Tanks	Ea	5	0.07	12	0.035
Powered N_2 Valves	Ea	15	0.05	36	0.02
N_2 Check Valves	Ea	10	0.01	24	0.005
Turbine Flow Meter + Gauge	Ea	5	0.06	12	0.025
Orifice Flow Meter + Gauge	Ea	5	0.02	12	0.005
Pressure Gauge	Ea	10	0.01	24	0.005

TABLE 4-4. (Continued)

Component or Item	Cost/ft^2 ($) Unit	Size or No. Required	Next Unit 100,000 ft^2	Size or No. Required	Cost/ft^2 Comm. Unit 10^6 ft^2
Pump Flex Connectors	Ea	30	0.01	72	0.005
Fluid Level Sensors	Ea	10	0.02	24	0.005
Air Selenoid Control Valves	Ea	30	0.01	72	0.005
Subtotal			0.56		0.255
Pipewelding & Instal.	Lot	-	1.50	-	1.00
Pipe Insulation	Lot	-	1.00	-	0.75
Bypass Lines	Not Needed		-	-	-
Subtotal			2.50		1.75
Total			25.75		14.00
Equals			277.07/m^2		150.64/m^2

TABLE 4-5
SUMMARY OF ITEMIZED COMPONENT COSTS FOR THE
NEXT PLANT AND A COMMERCIAL PLANT

Item or Task	Unit	Size or No. Required	Cost/ ft^2 100,000 ft^2	Size or No. Required	Cost/ ft^2 10^6 ft^2
Primary Concentrator	Module	∿330	8.00	∿3,300	3.40
Installation in Field	Module	∿330	3.35	∿3,300	1.60
Support Structure	Set	∿350	3.33	∿3,500	1.94
S.S. Installation	Set	∿350	0.87	∿3,500	0.56
Receiver Fabrication	Ea	∿330	5.55	∿3,300	3.34
Fluid System	Lot	-	0.56	-	0.255
F.S. Installation & Insulation	Lot	-	2.50	-	1.75
Control System	Ea	1	0.50	M-S sets	0.40
C.S. Installation & Checkout	Lot	-	1.09	-	0.755
Total			25.75		14.00
Equals			277.07/m^2		150.64/m^2

Table 4-4 gives the actual hardware costs; however, the cost of a project would be higher since the costs of management, engineering, testing, and tooling are not included. These can be significant, especially for the next plant, although they would drop progressively as commercialization takes place. The tooling consists primarily of the precision forms for casting the concrete modules. These costs are given in Table 4-6 for both the next plant and the commercial plant. A fee or profit allowance is not included in these totals.

TABLE 4-6
MAJOR FUNCTION COST SUMMARY FOR THE 100,000 FT^2
NEXT PLANT AND 1,000,000 FT^2 COMMERCIAL PLANT

Function and Tooling	100,000 Sq Ft Plant		1,000,000 Sq Ft Commercial Plant	
	Total Cost	Cost/Sq Ft	Total Cost	Cost Sq Ft
Management - Direct	250,000	2.50	583,560	0.58
(1 yr schedule) Off-Site Expenses	50,000	0.50	400,000	0.40
Engineering - Design	250,000	2.50	250,000	0.25
A and E	100,000	1.00	500,000	0.50
Preconstruction Testing	161,000	1.61	250,000	0.25
Module Form Fabrication	700,000	7.00	15,000,000	0.56
No. of Forms	10	Project bears full cost	300	Amortized over 3 yr, or 300 modules
Subsystem Fab. and Install (from Table 2.3)	2,750,000	25.75	14,000,000	14.00
Startup and Preoperation Testing	80,000	0.80	1,000,000	1.00
Total	4,166,000	41.66	17,540,000	17.54
Equals		448.26/m^2		188.73/m^2

ACKNOWLEDGMENT

General Atomic Company would like to express its appreciation for the capable support and fine cooperation of all Sandia personnel associated with this project. Both parties pursued the common goal of developing the effective utilization of solar energy for the purpose of adding an additional source to the nation's energy resources. General Atomic compliments Sandia's expertise and thanks them for their very helpful cooperation.

REFERENCES

1. Eggers, G. H., et al., "Solar Collector Field Subsystem Program on the Fixed Mirror Solar Concentrator - Final Report for the Period March 28, 1976, through September 30, 1976," DOE Report GA-A14209 (REV), General Atomic Company, December 31, 1976.
2. Eggers, G. H., et al., "Solar Collector Subsystem Program on the Fixed Mirror Solar Concentrator - Design and Tests," DOE Report GA-A14595, General Atomic Company, August 1977.
3. Eggers, G. H., "Operating Procedure and Maintenance Manual for the General Atomic FMSC Collector Subsystem at Sandia Laboratories," General Atomic Report GA-A15165, October 1978.

APPENDIX A

GENERAL ATOMIC RECEIVER TUBE CERTIFICATION

(Conducted by G. D. Miller and R. B. Pettit)

Sandia personnel were at Highland Plating Company in Los Angeles, California, on October 6 and 7, 1977, to certify the tubes being plated for General Atomic.

The measurements were performed using a Mobile Solar reflectometer, Model MS-251, and an infrared reflectometer, Model DB-100. Both instruments are manufactured by Gier-Dunkle Instruments, Inc. The tubes were sand-blasted at Highland Plating prior to plating. They were then plated with approximately 0.0127 mm (0.5 mils) of Harshaw dull nickel (similar to Watts nickel). The black chrome plating was done in new 3.81 m long (12½ ft) tanks. The numbered tubes were 3.7592 m (12 ft 4 in.) long. The lettered tubes were 3.8354 m (12 ft 7 in.) long, and because of the length had to be canted in the bath. The tubes numbered SP-1 through SP-5 were spare tubes without any fittings, and they were 12 ft long. The plating bath temperature was maintained at 13.3°C (56°F) during all plating operations. None of the tubes were wiped after plating.

While Miller was present at Highland, thirty tubes out of a total of 36 were completed. The numbered tubes were plated two at a time, while the lettered tubes were done one at a time.

The numbered tubes were plated for four and one-half minutes at a current density of 150 amps per square foot, and the lettered tubes were plated for four minutes and fifteen seconds. The current density for the lettered tubes was just short of 150 A.S.F. Before the plating conditions were finalized, several other times and currents were tried. Typical results are shown in Table A-1.

The first four tubes were checked for uniformity of the coating. (Refer to Table A-2 for uniformity data.) The remainder of the tubes were measured only in the center and opposite the stamped number or letter.

The average value for alpha was $\alpha_s = 0.97 \pm 0.008$, and the average total hemispherical emittance was $\varepsilon_{TH}(100°C) = 0.16 \pm 0.011$ and $\varepsilon_{TH}(300°C) = 0.23 \pm 0.014$. Table A-3 gives the complete data for individual tubes.

ABSORPTANCE MEASUREMENTS

The solar absorptance, α_s, is determined using a Gier-Dunkle Solar Reflectometer, Model MS-251. In order to obtain accurate α_s values, this instrument is calibrated to offset the effects of pipe geometry (as required) and intrinsic zero offset in the instrument. The overall accuracy of this measurement is ±0.03 absorptance units for electro-deposited black chrome coatings. The error may be larger for other coatings.*

*R. B. Pettit, "Optical Measurement Techniques Applied to Solar Selective Coatings," Sandia Report SAND-77-0421, August 1977.

TABLE A-1
TYPICAL CURRENT DENSITY, α, ε VALUES
FOR SOME OTHER PLATING CONDITIONS

Time	Current A.S.F.	C.D.	α	ε_{TH}(100°C)	ε_{TH}(300°C)
8 min	150	1200	0.98	0.18	0.26
7 min	155	1085	0.98	0.18	0.26
5 min	150	750	0.98	0.18	0.25
4 min	150	600	0.96	0.15	0.21

TABLE A-2
TABULATION OF UNIFORMITY DATA

Pipe	Position (See Fig. A-1)	α_s	ε_{TH}(100°C)	ε_{TH}(300°C)
3	1	0.981	0.18	0.26
3	2	0.981	0.18	0.26
2	1	0.959	0.15	0.21
2	2	0.958	0.15	0.20
9	1	0.975	0.18	0.24
9	2	0.975	0.17	0.25
11	1	0.970	0.18	0.25
11	2	0.970	0.18	0.25

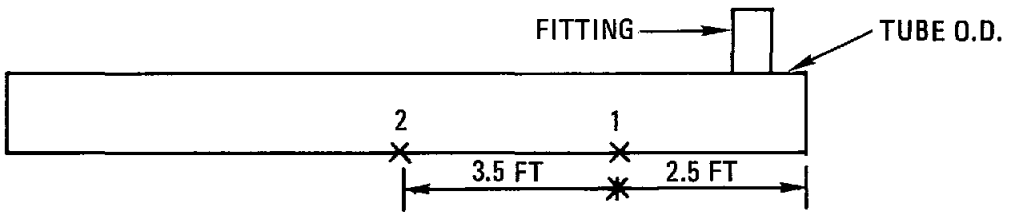

Figure A-1. Location of measurements for uniformity check

EMITTANCE MEASUREMENTS

The emittance properties are determined using a Gier-Dunkle Infrared Reflectometer, Model DB-100. This instrument is also calibrated to account for pipe geometry as required. Three different measurement methods can be used: (1) In the normal operating mode for this instrument, a polyethylene filter is in the optical path. This produces a measurement spectrum corresponding to a room temperature (∿25°C) blackbody. (2) By removing the polyethylene filter from the optical path, the measurement spectrum corresponds to a 100°C blackbody. (3) By inserting a sapphire filter in the optical path, the measured emittance corresponds to a temperature of 300°C for a black chrome coating only. The overall accuracy of this measurement is generally better than ±0.02 emittance units (Pettit).

TABLE A-3
TABULATION OF DATA

Pipe I.D.	α_s	ε_{TH}(100°C)	ε_{TH}(300°C)	Plating Order
SP-1	0.98	0.18	0.25	9
SP-2	0.98	0.18	0.25	10
SP-3	0.98	0.17	0.25	11
SP-4	0.97	0.17	0.24	12
SP-5	0.96	0.16	0.22	13
1	0.97	0.17	0.24	7
2	0.96	0.15	0.21	3
3	0.96	0.16	0.22	4
4	0.97	0.15	0.21	29
5	0.97	0.17	0.23	5
6	0.97	0.16	0.23	14
7	0.97	0.17	0.24	8
8	0.96	0.15	0.22	17
9	0.98	0.17	0.25	1
10	0.97	0.15	0.23	15
11	0.97	0.18	0.25	2
12	0.97	0.19	0.25	6
A	0.96	0.15	0.21	20
C	0.96	0.16	0.22	25
D	0.97	0.17	0.23	27
F	0.95	0.16	0.22	19
I	0.97	0.17	0.24	21
J	0.96	0.15	0.22	24
K	0.96	0.15	0.21	26
M	0.97	0.15	0.22	22
N	0.95	0.17	0.23	18
O	0.96	0.15	0.21	30
P	0.96	0.15	0.21	23
S	0.97	0.16	0.23	16
T	0.97	0.16	0.22	28

APPENDIX B

INCIDENT REPORT

FOR FIRST INCIDENT OCCURRING ON THE FMSC COLLECTOR SUBSYSTEM

INCIDENT

On December 9, 1977, the ball screw on the third receiver tracking jack from the west end of the General Atomic quadrant broke, allowing two receivers to fall. This jack is located at the west drive transfer pulley of the north row of collectors.

CAUSE

The mounting bracket for this jack is also the mounting for the drive tube pillow block of the primary drive train. The force for moving the receiver is transferred from the primary drive train to the secondary drive train at this point and one other point on the east end. There was an error on the fabrication drawing for this mounting bracket, and, therefore, the bracket would not fit as it was designed to. As a result a field change was made on this bracket and three others like it. This change involved cutting away part of the pillow block mounting plate. On three of the plates, the change made the bracket fit properly with adequate clearance, but on one of the brackets a step was left which could hang on the supporting mounting plate. When the bracket was installed and tested, it appeared to function properly, and the receiver traversed its full arc at least three times without any apparent malfunction. At the time of failure, the receiver was being driven down, i.e., to the south after being in the focal line further to the north. Examination of the mounting pad showed that the step in the cutaway had caught the supporting plate, bending the jack as it approached its highest point. The jack then could not rotate upward to follow the

screw motion. The screw then was forced into a curve, which caused it to break off at the jack.

RELATED DAMAGE

Potentially the greatest damage would be to the receiver pipe, which was twisted and warped as the result of falling. Particularly, the Marmon clamp flanges would be expensive and time consuming to repair if they were bent. The supporting blocks were bent and one receiver pillow block broke. The pump was turned off at the time of the incident so only a small amount of oil was spilled.

ACTION

The jack mounting bracket was removed and the step that caused the binding was cut out. The bracket was replaced with better shims that guarantee that the jack mounting bracket is centered in its supporting mounting plate. The shims were also replaced in the other three brackets, which were also carefully inspected for a possible recurrence of this incident.

CONCLUSION

This incident occurred during the initial checkout of the north row of collectors. It is not clearly understood why this jack mounting bracket initially operated without any observed malfunction, and then suddenly caught to cause damage. One tenable explanation is the rather large [0.95 cm (3/8 in.)] temperature expansion cycle of the aluminum drive tubes. Since there was room for side motion of the jack mounting bracket, the expansion of the drive tube could have pushed it over just enough to catch. The day was warm and the expansion of the tubes may have been slightly more than the previous time the receiver was operated. The new spacers will distribute this expansion along the drive assembly and prevent binding of the jack mounting bracket.

This is a brand new system, and there is no prior experience with either the engineering or the operation of this system. Personnel working with or around this system are urged to maintain an alert and vigilant inspection of its operation so as to spot possible malfunctions prior to damage occurring.

APPENDIX C

INCIDENT REPORT

FOR SECOND INCIDENT OCCURRING ON THE FMSC COLLECTOR SUBSYSTEM

INCIDENT

While the General Atomic collector subsystem was in operation on July 17, one of the jackscrews supporting the receivers on the south row failed. The failure allowed two of the eight receivers on the south row to begin falling. The undamaged receiver supports at the ends of the falling receivers were unable to support the momentum of the receivers and failed also. This led to the collapse of the entire south row of receivers in a domino fashion. In the process, the fluid seals between receivers were ruptured and approximately 20 gallons of Therminol 66 at 310°C (590°F) was spilled onto the ground. The spilled therminol quickly cooled to a temperature below its flash point, which eliminated the fire hazard. The therminol was quickly covered with an absorbent material to stop it from spreading.

CAUSE

The jackscrew that failed has been disassembled and inspected. No broken parts were found. The screw shaft, which had freed itself from the jack housing, was not damaged and screwed freely back into the worm gear. Upon examination, it was found that the key that locks the screw shaft to the worm gear had worked loose and fallen free. The screw shaft is threaded into the worm gear. So, without the locking key the worm gear drove the screw shaft out of its housing. This allowed the first receiver support to start falling. Since the neighboring receiver supports were not designed to support the momentum of a falling receiver tube, they failed also and the chain reaction began.

RELATED DAMAGE

The damage to the receivers consisted of bent Marmon clamp flanges at the ends of the absorber tubes and Teflon windows over the absorbers contaminated with Therminol 66. The receiver supports, along with their pillow block bearings, were all broken. One of the jack screw shafts was bent.

ACTION

A factory representative from the company that built the jackscrews was called in to examine the jackscrew that failed. He found that the locking key had worked loose and fallen free because an assembly operation that "should have been done at the factory" had been omitted. After the locking key is driven into its hold, the edge of its hole should have been peened over to lock the key in place. Each of the remaining 17 jackscrews in the collector system were checked and only one had its locking key properly installed. The jackscrews have all been fixed and reassembled.

The north (undamaged) collector string has been "red tagged" and will not be operated until a strengthened receiver support assembly has been designed, fabricated, and installed.

A Sandia estimate of the time and money required to bring the full system back to operational status and incorporate changes necessary to ensure against a recurrence has been prepared. A total of $25,000-$30,000 and 3 to 4 months will be required. General Atomic is providing a formal estimate of the repair costs, plus an estimate of upgrading the north string only.

DISTRIBUTION

TID-4500-R66, UC-62 (268)

Aerospace Corporation
101 Continental Blvd.
El Segundo, CA 90245
Attn: Elliott L. Katz

Solar Total Energy Program
American Technological University
P. O. Box 1416
Killeen, TX 76541
Attn: B. L. Hale

Argonne National Laboratory (3)
9700 South Cass Avenue
Argonne, IL 60439
Attn: R.G. Matlock
W.W. Schertz
Roland Winston

Battelle Memorial Institute
Pacific Northwest Laboratory
P. O. Box 999
Richland, WA 99352
Attn: K. Drumheller

Brookhaven National Laboratory
Associated Universities, Inc.
Upton, LI, NY 11973

Edison Electric Institute
90 Park Avenue
New York, NY 10016
Attn: L. O. Elsaesser,
Director of Research

Energy Institute
1700 Las Lomas
Albuquerque, NM 87131
Attn: T. T. Shishman

EPRI
3412 Hillview Avenue
Palo Alto, CA 94303
Attn: J. E. Bigger

Georgia Institute of Technology
Atlanta, GA 30332
Attn: J. D. Walton

Georgia Power Company
Atlanta, GA 30302
Attn: Mr. Walter Hensley
Vice President Economics Services

Jet Propulsion Laboratory
4800 Oak Grove Drive
Pasadena, CA 91103
Attn: V. C. Truscello

Lawrence Berkeley Laboratory
University of California
Berkeley, CA 94720
Attn: Mike Wallig

Lawrence Livermore Laboratory
University of California
P. O. Box 808
Livermore, CA 94500
Attn: W. C. Dickinson

Los Alamos Scientific Laboratory (2)
Los Alamos, NM 87545
Attn: J. D. Balcomb
D. P. Grimmer
C. D. Bankston

NASA-Lewis Research Center
Cleveland, OH 44135
Attn: R. Hyland

New Mexico State University
Solar Energy Department
Las Cruces, NM 88001

Oak Ridge National Laboratory (4)
P. O. Box Y
Oak Ridge, TN 37830
Attn: J. R. Blevins
C. V. Chester
J. Johnson
S. I. Kaplan

Office of Technology Assessment
U. S. Congress
Washington, DC 20510
Attn: Dr. Henry Kelly

PRC Energy Analysis Co.
7600 Old Spring House Rd.
McLean, VA 22102
Attn: K. T. Cherian

Solar Energy Research Institute (9)
1536 Cole Blvd.
Golden, CO 80401
Attn: C. J. Bishop
Ken Brown
B. L. Butler
Frank Kreith
Charles Grosskreutz
B. P. Gupta
A. Rabl
Library, Bldg No. 4 (2)

Southwest Research Institute
P. O. Box 28510
San Antonio, TX 78284
Attn: Danny M. Deffenbaugh

U. S. Department of Energy
Agricultural & Industrial
Process Heat
Conservation & Solar Application
Washington, DC 20545
Attn: W. W. Auer
J. Dollard

U. S. Department of Energy (3)
Albuquerque Operations Office
P. O. Box 5400
Albuquerque, NM 87185
Attn: D. K. Nowlin
G. Pappas
J. R. Roder

U. S. Department of Energy
Division of Energy Storage Systems
Washington, DC 20545
Attn: C. J. Swet

U. S. Department of Energy (9)
Division of Central Solar Technology
Washington, DC 20545
Attn: R. H. Annan
G. W. Braun
H. Coleman
M. U. Gutstein
G. M. Kaplan
Lou Melamed
J. E. Rannels
M. E. Resner
J. Weisiger

U. S. Department of Energy
Los Angeles Operations Office
350 S. Figueroa Street, Suite 285
Los Angeles, CA 90071
Attn: Fred A. Glaski

U. S. Department of Energy
San Francisco Operations Office
1333 Broadway, Wells Fargo Bldg.
Oakland, CA 94612
Attn: Jack Blasy

University of Delaware
Institute of Energy Conversion
Newark, DE 19711
Attn: K. W. Boer

University of New Mexico (2)
Department of Mechanical Eng.
Albuquerque, NM 87113
Attn: W. A. Cross
M. W. Wilden

2323	C. M. Gabriel
2324	L. W. Schulz
2326	G. M. Heck
4700	J. H. Scott
4710	G. E. Brandvold
4713	B. W. Marshall
4714	R. P. Stromberg
4715	R. H. Braasch
4719	D. G. Schueler
4720	V. L. Dugan
4721	J. V. Otts
4721	L. E. Torkelson (20)
4722	J. F. Banas
4723	W. P. Schimmel
4725	J. A. Leonard
5512	H. C. Hardee
5830	M. J. Davis
5840	H. J. Saxton
5844	F. P. Gerstle
8450	R. C. Wayne
8453	J. D. Gilson
8266	E. A. Aas
3141	T. L. Werner (5)
3151	W. L. Garner (3)
	For DOE/TIC
	(Unlimited Release)